

This discussion paper is/has been under review for the journal Earth System Dynamics (ESD). Please refer to the corresponding final paper in ESD if available.

Differential climate impacts for policy-relevant limits to global warming: the case of 1.5 °C and 2 °C

C.-F. Schleussner^{1,2}, T. K. Lissner^{1,2}, E. M. Fischer³, J. Wohland², M. Perrette², A. Golly^{4,6}, J. Rogelj^{3,5}, K. Childers², J. Schewe², K. Frieler², M. Mengel^{1,2}, W. Hare^{1,2}, and M. Schaeffer^{1,7}

¹Climate Analytics, Friedrichstr 231 – Haus B, 10969 Berlin, Germany

²Potsdam Institute for Climate Impact Research, Potsdam, Germany

³Institute for Atmospheric and Climate Science, ETH Zurich, Zürich, Switzerland

⁴GFZ German Research Centre for Geosciences, Potsdam, Germany

⁵Energy Program, International Institute for Applied Systems Analysis, Laxenburg, Austria

⁶University of Potsdam, Institute of Earth and Environmental Science, Potsdam, Germany

⁷Wageningen University and Research Centre, Environmental Systems Analysis Group, Wageningen, the Netherlands

Received: 8 October 2015 – Accepted: 11 November 2015 – Published: 27 November 2015

Correspondence to: C.-F. Schleussner (carl.schleussner@climateanalytics.org)

Published by Copernicus Publications on behalf of the European Geosciences Union.

Title Page

Abstract

Introduction

Conclusions

References

Tables

Figures



Back

Close

Full Screen / Esc

Printer-friendly Version

Interactive Discussion



Abstract

Robust appraisals of climate impacts at different levels of global-mean temperature increase are vital to guide assessments of dangerous anthropogenic interference with the climate system. Currently, two such levels are discussed in the context of the international climate negotiations as long-term global temperature goals: a below 2°C and a 1.5°C limit in global-mean temperature rise above pre-industrial levels. Despite the prominence of these two temperature limits, a comprehensive assessment of the differences in climate impacts at these levels is still missing. Here we provide an assessment of key impacts of climate change at warming levels of 1.5°C and 2°C, including extreme weather events, water availability, agricultural yields, sea-level rise and risk of coral reef loss. Our results reveal substantial differences in impacts between 1.5°C and 2°C. For heat-related extremes, the additional 0.5°C increase in global-mean temperature marks the difference between events at the upper limit of present-day natural variability and a new climate regime, particularly in tropical regions. Similarly, this warming difference is likely to be decisive for the future of tropical coral reefs. In a scenario with an end-of-century warming of 2°C, virtually all tropical coral reefs are projected to be at risk of severe degradation due to temperature induced bleaching from 2050 onwards. This fraction is reduced to about 90% in 2050 and projected to decline to 70% by 2100 for a 1.5°C scenario. Analyses of precipitation-related impacts reveal distinct regional differences and several hot-spots of change emerge. Regional reduction in median water availability for the Mediterranean is found to nearly double from 9 to 17% between 1.5°C and 2°C, and the projected lengthening of regional dry spells increases from 7% longer to 11%. Projections for agricultural yields differ between crop types as well as world regions. While some (in particular high-latitude) regions may benefit, tropical regions like West Africa, South-East Asia, as well as Central and Northern South America are projected to face local yield reductions, particularly for wheat and maize. Best estimate sea-level rise projections based on two illustrative scenarios indicate a 50 cm rise by 2100 relative to year 2000-levels

Climate impacts at 1.5°C and 2°C

C.-F. Schleussner et al.

Title Page

Abstract

Introduction

Conclusions

References

Tables

Figures



Back

Close

Full Screen / Esc

Printer-friendly Version

Interactive Discussion



under a 2°C warming, which is about 10 cm lower for a 1.5°C scenario. Our findings highlight the importance of regional differentiation to assess future climate risks as well as different vulnerabilities to incremental increases in global-mean temperature. The article provides a consistent and comprehensive assessment of existing projections and a solid foundation for future work on refining our understanding of warming-level dependent climate impacts.

1 Introduction

Recent decades have seen increasing climate impacts, many of which science is now able to attribute to anthropogenic carbon dioxide emissions and consequent global warming (IPCC, 2013; King et al., 2015). On-going temperature increase will escalate these impacts on ecological and human systems (IPCC, 2014a), which has made climate change a political issue of utmost importance. Already in 1992, the international community established the United Nations Framework Convention on Climate Change (UNFCCC) with the objective of a “stabilization of greenhouse gas concentrations in the atmosphere at a level that would prevent dangerous anthropogenic interference with the climate system” (UNFCCC, 1992). The extent and level of such a “dangerous anthropogenic interference”, however, remains a topic of debate until today.

To operationalize this convention in terms of a long-term global temperature goal to guide mitigation action, the parties under the UNFCCC agreed in 2010 “to hold the increase in global average temperature below 2°C above pre-industrial levels” (UNFCCC, 2010), while recognizing the need to review this goal on the basis of the best available science and exploring limiting global temperature increase to 1.5°C (UNFCCC, 2010). A recent expert assessment reviewing the adequacy of the long-term global goal concluded that “significant climate impacts are already occurring [...] and additional magnitudes of warming will only increase the risk of severe, pervasive and irreversible impacts” (SED, 2015), stressing the fact that 2°C of global warming should be seen as an upper limit, and not a “safe” limit. While a below 2°C-goal

Title Page

Abstract

Introduction

Conclusions

References

Tables

Figures



Back

Close

Full Screen / Esc

Printer-friendly Version

Interactive Discussion



has been agreed politically, scientific evidence indicates that severe and potentially irreversible impacts of climate change may already occur for lower levels of warming (IPCC, 2014a). As yet, such evidence remains fragmented, and comprehensive, multi-sectoral assessments of differences in climate impacts between a 1.5°C and 2°C temperature increase are lacking.

The “Turn down the heat” – report series issued by the World Bank (Schellnhuber et al., 2012, 2013, 2014) assessed climate risks for a 2°C and a 4°C warming above pre-industrial levels for different world regions. The report of the Working Group 2 (WG2) of the Fifth Assessment Report (AR5) of the Intergovernmental Panel on Climate Change (IPCC) includes both, chapters on specific impacts as well as on specific regions, and provides warming level dependent information on impacts where available. The range of emission scenarios which provide the basis for the climate impact projections in the IPCC AR5, the Representative Concentration Pathways (RCPs), however, do not allow for a straight-forward differentiation between impacts for warming levels of 1.5°C and 2°C. Only the lowest emission pathway RCP 2.6 is in line with keeping global-mean surface–air temperature (GMT) increase above pre-industrial levels to below 2°C with a likely chance (66 % probability, IPCC, 2013) and no pathway in line with a 1.5°C limit is assessed. Still, the IPCC AR5 WG2 report provides an expert assessment of key impacts at different levels of warming, summarized in five “Reasons-for-Concern” (RFCs, Oppenheimer et al., 2014). The risks for three out of five of these RFCs are assessed as at least moderate at 1.5°C GMT increase above pre-industrial levels, and as high at 2°C. Moderate risks hereby mean that associated impacts are both detectable and attributable to climate change with at least medium confidence, whereas high risks are associated with severe and widespread impacts (Oppenheimer et al., 2014). Among the three RFCs that show high risks at 2°C are *Risks to unique and threatened systems* (RFC1) that include coral reefs and other highly vulnerable human systems as well as ecosystems, *Risks associated with extreme weather events* (RFC2) and *Risks associated with the distribution of impacts* (RFC3).

**Climate impacts at
1.5°C and 2°C**

C.-F. Schleussner et al.

Title Page

Abstract

Introduction

Conclusions

References

Tables

Figures



Back

Close

Full Screen / Esc

Printer-friendly Version

Interactive Discussion



**Climate impacts at
1.5 °C and 2 °C**

C.-F. Schleussner et al.

Title Page

Abstract

Introduction

Conclusions

References

Tables

Figures



Back

Close

Full Screen / Esc

Printer-friendly Version

Interactive Discussion



Based on the data archives of the Coupled Model Intercomparison Project 5 (CMIP5, Taylor et al., 2011) and the Inter-Sectoral Impact Model Intercomparison Project (ISI-MIP, Warszawski et al., 2013), this article provides an extensive assessment of regionally differentiated climate impacts at levels of 1.5 °C and 2 °C global mean surface–air temperature increase (GMT) above pre-industrial levels (hereinafter 1.5 °C and 2 °C) for different climate impacts, including increases in climatic extremes (Sect. 3), changes in water availability (Sect. 4), crop yield projections (Sect. 5), sea-level rise (SLR, Sect. 6) and coral reef degradation (Sect. 7).

The following Sect. 2 outlines the common methodological approach taken for the assessment of changes in climate extremes, water availability and agricultural impacts. Consequently, regionally differentiated results for the specific impacts listed above at 1.5 °C and 2 °C warming are presented. Analyses of sea-level rise and impacts on coral reefs contain additional details on sector-specific methods. Where impact-specific additional methodological specifications are needed, these are given in the respective section, followed by a presentation of the main results and a short discussion. A summarizing discussion as well as some conclusions finalize this contribution in Sect. 8. The Supplement provides additional methodological information as well as further impact maps and summary impact tables.

2 Methods

This section provides an overview of the methods applied for the assessment of climate extremes, water availability and agricultural impacts. The individual subsections provide additional information on sector- and impact-specific methods as well as on the data analyzed. The meteorological extreme indices are derived from an ensemble of general circulation models (GCMs) of CMIP5 (Taylor et al., 2011) while our assessment of water availability and agricultural impacts at 1.5 °C and 2 °C is based on the ISI-MIP Fast Track data (Warszawski et al., 2013; Frieler et al., 2015).

**Climate impacts at
1.5 °C and 2 °C**

C.-F. Schleussner et al.

Title Page

Abstract

Introduction

Conclusions

References

Tables

Figures



Back

Close

Full Screen / Esc

Printer-friendly Version

Interactive Discussion



For both data archives, the impacts for a GMT increase of 1.5 °C and 2 °C above pre-industrial levels are derived for 20-year time slices around the respective time-averaged warming for each model separately. To account for model deviations from observations over the historical period, the warming levels are derived relative to the reference period 1986–2005, (this reference period lies 0.6 °C above pre-industrial levels, IPCC, 2013), which translates to a warming of 0.9 °C and 1.4 °C above reference period levels for the 1.5 °C and 2 °C limit, respectively. All time slices are derived from the RCP8.5 scenario (the time slices for the individual GCMs are given in Table S1 in the Supplement). 1986–2005 is also the common reference period to assess projected changes in extreme indices and and climate impacts. Therefore, where results speak of impacts at 1.5 °C and 2 °C, the GMT increase refers to pre-industrial temperature, while the impact signal is derived relative to the reference period.

Analyzing time-slices centered around a specific level of warming relies on the assumption that the changes in the climate and climate impact signals studied here are dominantly driven by changes in GMT and that the effect of changes in time-lagged systems such as large-scale ocean circulations (Schleussner et al., 2014, 2013) on the quantities studied are of minor importance. In addition, this approach does not account for the effect of other anthropogenic climate forcings that may differ for the same level of total radiative forcing such as aerosols (Zopa et al., 2012). It comes, however, also with several advantages. In particular, it eliminates the spread due to different transient climate responses across the model ensemble, which can deviate by up to a factor of two (Flato et al., 2013). Traditional approaches that analyze impacts over a given time period for all models in a model ensemble and relate this to a median GMT increase across the model ensemble do not account for this ensemble-intrinsic spread of global warming levels and will consequently overestimate the ensemble uncertainty of the GMT-dependent indices studied.

In addition to the anthropogenic forcing, natural variability is a dominant driver of the climate signal on multi-annual time scales for time-averaged quantities such as mean temperature and precipitation change (Knutti and Sedláček, 2012; Marotzke

Climate impacts at 1.5 °C and 2 °C

C.-F. Schleussner et al.

Title Page

Abstract

Introduction

Conclusions

References

Tables

Figures



Back

Close

Full Screen / Esc

Printer-friendly Version

Interactive Discussion



and Forster, 2014) and in particular for extreme events (Kendon et al., 2008; Tebaldi et al., 2011). This finding has been further consolidated by perturbed-initial condition ensemble simulations (Fischer et al., 2013). Thus, natural variability may mask the effect of climate change on an individual grid cell basis and consequently lead to a delayed detection of the imprints of climate change (Tebaldi and Friedlingstein, 2013). To overcome this limitation, Fischer et al. (2013) have proposed a spatial aggregation approach that allows for a robust detection of changes in climatic extremes despite the substantial effect of natural variability on an individual grid-cell level – an approach that has also been successfully applied to the observational record (Fischer and Knutti, 2014). Here, we adopt and extend this spatial aggregation approach.

As in Fischer et al. (2013), we consider the distribution of changes in the selected impact indicator at each grid point over the global land-mass between 66° N and 66° S (for the sake of simplicity henceforth referred to as global land-mass) and additionally analyze changes for 26 world regions (as used in IPCC, 2012, see Table 1 for details). This yields distributions for 1.5 °C and 2 °C for each of the ensemble members and regions, where the sample size is given by the number of grid points included. This allows for a pair-wise assessment using a two-sample Kolmogorov–Smirnov (KS) test with the null hypothesis that both distributions for 1.5 °C and 2 °C are drawn from the same probability distribution.

A rejection of the test's null-hypothesis at a significance level of 95 % indicates a robust difference in projections between these two warming levels. This pairwise test, based on the individual models used for the assessment, allows for robust statements about differences in impacts between the two warming levels, even if there is substantial overlap of uncertainty bands in the model ensemble. For GCMs that provide multiple realizations, the distributions are combined for each warming level leading to larger samples and higher discriminatory power of the KS test. Please note that this approach is only applied for the KS test and not for the ensemble projections. For the latter, the averaged signal over multiple realizations of a single GCM is included in the ensemble analysis ensuring equal weight to all GCMs investigated (see Sect. S1

in the Supplement for further detail on the methodology applied and the treatment of multiple realizations). A similar approach has been applied recently to investigate the timing of anthropogenic emergence in simulated climate extremes (King et al., 2015).

Based on the regionally specific distributions, cumulative density functions (CDF) of changes in the impact over the land area of the respective region are derived. As in Fischer et al. (2013), we fit a probability density function to the empirical distribution of the climate signal using a Gaussian kernel density estimator. Individual grid-cells are weighted according to their latitude-dependent area. These CDFs are derived for each ensemble member (GCM or GCM-impact model combination) and the ensemble median as well the likely range (66 % of the ensemble members are within this range) are given. This land-area focused approach allows to directly assess not only the median change over a region, but also changes for smaller fractions of the land area. At the same time, the uncertainty estimates based on the model ensemble spread can be directly visualized.

3 Climate extremes indices

There is a growing body of evidence showing that the frequency and intensity of many climatic extremes has increased significantly over the last decades as a result of anthropogenic climate change, but confidence in the significance of the trend and attribution to anthropogenic origin differ substantially between types of extreme weather events and regions (IPCC, 2013). With on-going warming, these trends are projected to continue (IPCC, 2012). Impacts of climate extremes will particularly, but not exclusively, affect the most vulnerable with the lowest levels of adaptive capacity and represent one of the biggest threats posed by climate change (IPCC, 2014b). In this Section, the difference in impacts between a warming of 1.5°C and 2°C for four different types of meteorological extreme event indices are assessed. The definition of these indices follow the recommendations of the Expert Team on Climate Change Detection and Indices (Zhang et al., 2011) and are derived on an annual basis:

Title Page

Abstract

Introduction

Conclusions

References

Tables

Figures



Back

Close

Full Screen / Esc

Printer-friendly Version

Interactive Discussion



- Intensity of hot extremes (TXx): annual maximum value of daily maximum temperature.
- Warm spell duration indicator (WSDI): annual count of the longest consecutive period in which the daily maximum temperature for each day exceeds the 90 % quantile for this day over the reference period. The minimum length is six consecutive days.
- Dry spell length or consecutive dry days (CDD): annual maximum number of consecutive days for which the precipitation is below 1 mm day^{-1} .
- Heavy precipitation intensity or maximum accumulated five-day precipitation (RX5day): absolute annual maximum of consecutive 5 day precipitation.

3.1 Methods and data

Projected changes in climate extreme indices are assessed using an 11-member model ensemble of CMIP5 for TXx and WSDI and a 14-member model ensemble of CMIP5 for RX5day and CDD, based on the methods outlined in Sect. 2. All available GCMs are assessed on a uniform grid with a $2.5^\circ \times 1.9^\circ$ resolution. Multiple realizations of scenario runs for individual models are included when available, and in that case allow to estimate CDFs for natural variability that are derived based on pairwise realizations of model runs over the reference period (see Sect. S1.2 for further detail on the methodology applied).

We assess the changes in TXx and WSDI for a warming of 1.5°C and 2°C and derive changes of 20-year averages of extreme indices for the model dependent warming-level time-slices at each land grid point relative to the 1986–2005 reference period. Changes in precipitation-related indices are described as relative changes while we consider absolute changes for the other indicators. For the CDF analysis for TXx, the absolute signal is normalized by the standard deviation over the reference period.

[Title Page](#)
[Abstract](#)
[Introduction](#)
[Conclusions](#)
[References](#)
[Tables](#)
[Figures](#)
[Back](#)
[Close](#)
[Full Screen / Esc](#)
[Printer-friendly Version](#)
[Interactive Discussion](#)


3.2 Results

3.2.1 Heat extremes

Substantial increases of 3°C and more in TXx over large parts of the Northern Hemisphere, Central South America and South Africa as well as increases in warm-spell durations (WSDI) of 3 months and more are projected under a warming of 2°C. Figure 1 depicts changes in TXx (left) and WSDI (right) for a 1.5°C (top) and 2°C (middle) GMT temperature increase, as well as the differences between the two warming levels (bottom) on a grid-cell basis. Particularly strong increases in WSDI are found in some tropical coastal areas, which we attribute to a large share of ocean surface in the respective grid cells that lead to an amplification of the effect compared to pure land grid cells and should not be over-interpreted. We excluded these grid-cells for the CDF analysis for the respective regions. The majority of GCMs agree on a robust increase in these heat-related indices and show significant differences between the two warming levels. The impacts are robustly smaller at 1.5°C warming in both cases (see results for the KS test listed in Table S2).

Globally and regionally resolved CDFs for TXx, normalized to the standard deviation (σ) over the reference period, are given in Fig. 2 and median values are listed in Table S2. 50% of the global land-mass will experience a median TXx increase of more than 1.2 (1.8) standard deviations relative to the reference period for a warming of 1.5°C (2°C) above pre-industrial levels. The regional assessments indicate that the tropical regions in Africa, South America and South East Asia are projected to experience the strongest increase in land area covered by heat extremes relative to the regional natural variability, where 3σ events become the new normal under a 2°C warming.

The pattern of a strong tropical signal is mainly due to the small natural variability of TXx in tropical regions. This is also apparent for the WSDI CDFs resolved in Fig. 3. For a warming of 1.5°C, a median increase in WSDI length by about one month is projected for 50% of the global land area that increases by 50% for a 2°C warming.

Title Page

Abstract

Introduction

Conclusions

References

Tables

Figures



Back

Close

Full Screen / Esc

Printer-friendly Version

Interactive Discussion



Climate impacts at 1.5 °C and 2 °C

C.-F. Schleussner et al.

Title Page

Abstract

Introduction

Conclusions

References

Tables

Figures



Back

Close

Full Screen / Esc

Printer-friendly Version

Interactive Discussion



Since this index is derived relative to natural variability over a reference period, the signal again is greatly amplified in tropical regions, where a median WSDI of up to three month is projected for Amazonia, East and West Africa and South-East Asia (see Table S2). Given that the WSDI only measures the longest consecutive interval, such an increase can be interpreted as entering a new climate regime for these tropical regions (Diffenbaugh and Scherer, 2011; Mora et al., 2013; King et al., 2015).

A meaningful assessment of impacts requires not only an assessment of absolute changes, but these also have to be interpreted in the light of regional climate conditions. It is the regional natural climate variability that determines a “climate normal” to which human systems as well as ecosystems are adapted (Hansen et al., 2012; Coumou and Robinson, 2013). While this may hold as a general assumption for a range of impacts concerning human health as well as ecosystems, it is important to note that the severity of certain climate impacts may also depend on the exceedance of absolute thresholds, as has been shown for temperature effects on crop yields, for example (Deryng et al., 2014; Smith et al., 2014). The choice of an either relative or absolute representation of changes in climate impacts thus has to be made in the light of the impact of interest.

Our findings are in line with previous assessments of projected changes in extreme temperatures and heat-waves (Orlowsky and Seneviratne, 2012; Sillmann et al., 2013; Kharin et al., 2013) and illustrate the substantial increase in the likelihood of heat extremes between 1.5 °C and 2 °C warming above pre-industrial levels, in particular when putting these changes in perspective to regional natural climate variability (Diffenbaugh and Scherer, 2011; Coumou and Robinson, 2013).

3.2.2 Extreme precipitation and dry spells

Uncertainty in model projections of precipitation extremes is considerably larger than that of temperature related extremes. Figure 4 depicts the median projections for RX5day (Maximum accumulated five-day precipitation, left) and CDD (Dry spell length, right), which exhibit contrasting patterns in terms of signal strength and robustness. The KS test reveals the additional merit of regional analysis of these precipitation-

related extremes (see Table S3). While all models in the ensemble indicate a robust difference between a 1.5 °C and 2 °C warming for both indices for the global land mass, the analysis for the separate world regions reveals different patterns.

A robust indication (more than 66 % of the models reject the null hypothesis of the KS test at the 95 % significance level, see Table S3) of a difference in RX5day is projected in particular for the high northern latitude regions, East Asia, as well as East and West Africa. While the high northern latitudes are also among those regions experiencing the largest increase in RX5day between the assessed warming levels (up to 7 and 11 %, median estimates for 1.5 °C and 2 °C, respectively), projections for other regions that experience a considerable increase under a 1.5 °C warming do not indicate a significant difference between the warming levels. This is in particular noteworthy for the Amazon region and North-East Brazil, where precipitation extremes are likely related to the South American monsoon systems (Boers et al., 2014) and to a lesser extent for West Africa (see Fig. 5 and Table S3).

A different picture emerges for CDD as an indicator for dry spell length. For the majority of the global land area, little to no differences in CDD are projected relative to the reference period (see Fig. 4). However, about 40 % of the global land area in the subtropical and tropical regions experience an increase in CDD length, including the Mediterranean, Central America, the Amazon as well as South Africa (compare Figs. 4 and 6). In these regions, the KS test also reveals robust indications for differences in impacts between 1.5 °C and 2 °C. This difference is particularly pronounced for the Mediterranean region, where the CDD length increases from 7 % (likely range 4–10 %) to 11 % (likely range 6–15 %) between 1.5 °C and 2 °C.

It is important to highlight that CDD is only an indicator for dry spell length and does not account for changes in evapotranspiration and soil-moisture related effects. It should hence not be interpreted as a direct indicator for agricultural or hydrological (streamflow) drought (Mueller and Seneviratne, 2012; Orłowsky and Seneviratne, 2012). Furthermore, CDD is a metric for short dry spells, which represent only a snapshot of the overall changes in dryness (IPCC, 2012), while high-impact

[Title Page](#)[Abstract](#)[Introduction](#)[Conclusions](#)[References](#)[Tables](#)[Figures](#)[Back](#)[Close](#)[Full Screen / Esc](#)[Printer-friendly Version](#)[Interactive Discussion](#)

Title Page

Abstract

Introduction

Conclusions

References

Tables

Figures



Back

Close

Full Screen / Esc

Printer-friendly Version

Interactive Discussion



drought events like the Big Dry in Australia (Kiem and Verdon-Kidd, 2010) or the ongoing California drought stretch over month and potentially years (Ault et al., 2014). Nevertheless, CDD as well as RX5day can be seen as proxies for the precipitation-related component when assessing drought and flooding risks, respectively, and the results and impacted regions identified here are broadly consistent with projections based on more comprehensive indicators for droughts (Dai, 2012; Prudhomme et al., 2013) and flooding risk (Hirabayashi et al., 2013) alike.

4 Water availability

Already today, water scarcity is among the biggest challenges for ecosystems and human societies in many regions globally. To assess changes in water availability (assessed here as the annual mean surface and subsurface runoff – QTOT) at 1.5 °C and 2 °C, we follow the approach outlined above in Sect. 2. Projections are based on 11 global hydrological models (GHM) forced with bias–corrected climate simulations from five GCMs (Hempel et al., 2013) used in ISI-MIP, as described in Schewe et al. (2013). Unlike for the CMIP5 ensemble, only one realization of each experiment is available and as a consequence the effect of natural variability cannot be assessed. ISI-MIP impacts are assessed at a 0.5° × 0.5° resolution.

4.1 Results

For a warming of 2 °C, reductions in water availability of up to 30 % are projected in several – mainly subtropical – regions, in particular affecting the Mediterranean, South Africa, Central and Southern South America and South Australia (Fig. 7). A relative increase in runoff is projected in much of the high northern latitudes, as well as in parts of India, East Africa and parts of the Sahel. While many of these findings are consistent with earlier studies (James and Washington, 2013; Schewe et al., 2013),

some may depend on the five GCMs chosen here and may be less robust in larger CMIP5 GCM ensembles (Knutti and Sedláček, 2012).

Figures 7 (lower panel) and 8 illustrate the difference between a 1.5°C and 2°C warming. Differences are most prominent in the Mediterranean region where the median reduction in runoff almost doubles from about 9% (likely range: 4.5–15.5%) at 1.5°C to 17% (8–28%) at 2°C. For several other world regions such as Central America and Australia, there is an increasing risk of substantial runoff reductions exceeding 30% for the upper limit of the 66% quantile, although projections are highly uncertain (Table S4 and Fig. 8). The differences between 1.5°C and 2°C are smaller for many other regions, but the KS-test reveals that they are statistically significant for all world regions assessed (Table S4). These runoff results are also consistent with the findings on precipitation related extremes presented in Sect. 3.2.2.

5 Assessing agricultural risks

5.1 Methods and data

To assess projections of future agricultural crop yields in a 1.5°C and 2°C warmer world, we base our analysis of climate change impacts on the yields for the four major staple crops maize, wheat, rice and soy in the ISI-MIP database (Warszawski et al., 2013; Rosenzweig et al., 2013). Projections for agricultural production depend on a complex interplay of a range of factors, including physical responses to soils, climate and chemical processes, or nutrient and water availability, but are also strongly determined by human development and management. The representation of these processes differs strongly between different agricultural models. While studies suggest an increase in productivity for some crops as a result of higher CO₂-concentrations, large uncertainties remain with regard to temperature sensitivity, nutrient and water limitations, differences in regional responses and also the interactions between those different factors (Rosenzweig et al., 2013). According to their metabolic pathways of

Title Page

Abstract

Introduction

Conclusions

References

Tables

Figures



Back

Close

Full Screen / Esc

Printer-friendly Version

Interactive Discussion



Climate impacts at 1.5 °C and 2 °C

C.-F. Schleussner et al.

Title Page

Abstract

Introduction

Conclusions

References

Tables

Figures



Back

Close

Full Screen / Esc

Printer-friendly Version

Interactive Discussion



carbon fixation in photosynthesis, main crops can be categorized as C3 and C4 plants. C4 plants such as maize, sorghum and sugar cane have a high CO₂ efficiency and as a consequence profit little from increased CO₂-concentrations, whereas for C3 plants including wheat, rice and soy a positive CO₂ – fertilization effect is to be expected.

At the same time, increased CO₂-concentrations may lead to improved water use efficiency (Eamus, 1991). However, the effect of elevated CO₂ concentrations on plant growth is highly uncertain (McGrath and Lobell, 2013) and the representation of this effect greatly differs between different agricultural models. As a consequence, the ISI-MIP protocol has been conducted with and without accounting for CO₂-fertilization effects (further referred to as the CO₂-ensemble and noCO₂-ensemble, respectively). Recent findings also underline the importance of elevated temperatures and heat extremes (Gourdji et al., 2013; Deryng et al., 2014), ozone concentrations (Tai et al., 2014) as well as the potential of increasing susceptibility to disease as a consequence of elevated CO₂ levels (Vaughan et al., 2014) for agricultural yields, which may counteract potential yield gains by CO₂-fertilization (Porter et al., 2014). Results for the CO₂ and noCO₂-ensembles are presented separately, showing the range of potential manifestations and the additional risks of regional yield reductions, if effects of CO₂-fertilization turn out to be lower than estimated by the model ensemble.

The ISI-MIP ensemble contains simulations based on seven Global Gridded Crop Models (GGCM) for wheat, maize and soy and six GGCM for rice, run with input from five CMIP5 GCMs (for further information see Rosenzweig et al., 2013). For the CO₂-ensemble, all model combinations are available (35, and 30 for rice), while for the noCO₂-ensemble runs have been provided for 23 (18 for rice) GGCM-GCM combinations. We restrict future crop growing areas (Monfreda et al., 2008) to present day agricultural areas and assume no change in management type, meaning that “rainfed” and “irrigation” conditions are kept constant as well.

As in previous sections, the results presented here are based on 20-year time slices from the RCP8.5 simulations and changes are given relative to the 1986–2005 reference period. The choice of displaying relative changes comes with several

advantages, but will also lead to a disproportional visual amplification of minor absolute changes for regions with small present day yields, in particular in the high northern latitudes. An overview of the regionally resolved present day share in global production is given in Fig. S5.

5 Since agricultural impacts depend both on climatological changes and changes in the atmospheric CO₂-concentrations, the assumption of time-independent impacts underlying the time-slice-approach as discussed above does not fully hold for agricultural projections accounting for the effects of CO₂-fertilization (the CO₂-ensemble) and will lead to increased inner-ensemble spread as a consequence. Please
10 note that the regional aggregation for agricultural yields is not based on absolute yield change but on land area, as for the other indicators studied above. Since societal impacts of changes in agricultural production go beyond mere changes in yield, but also include for example local livelihood dependencies (Schellnhuber et al., 2013; Olsson et al., 2014), our assessment of local yield changes (on a grid-cell level) supplements
15 and extends previous yield-centered analysis (Rosenzweig et al., 2013). Maps for the projected differences of yield changes on a grid-cell basis are provided in the Supplement.

5.2 Results

5.2.1 Wheat

20 Our analysis reveals very small local median yield changes for 50 % of the global land area for a 1.5 °C and 2 °C warming. However, the uncertainties of these projections are substantial and reductions of about 6 and 8 % for 1.5 °C and 2 °C, respectively, mark the lower end of the likely range (compare Table S5). For the noCO₂-ensemble, we find substantial median reductions in local wheat yields of 14 % at 1.5 °C, with
25 a statistically significant higher decrease of 19 % at 2 °C and potential reductions of up to 20 % (1.5 °C) and 37 % (2 °C) as lower limits for the likely range. The results of the KS-tests based on individual model combinations are given in Table S5 and for the

Title Page

Abstract

Introduction

Conclusions

References

Tables

Figures



Back

Close

Full Screen / Esc

Printer-friendly Version

Interactive Discussion



global level as well as most regions, more than 83 % (90 %) of all ensemble members indicate a robust difference between projected impacts at 1.5 °C and 2 °C for the CO₂ (noCO₂)-ensemble.

Local yield reductions are projected for most tropical regions. A median reduction of 13 % (19 %) is projected for 50 % of the West African agricultural area for 1.5 °C (2 °C) and more than 6 % for East Africa. Both, CO₂ and noCO₂-ensembles, project wheat yield increases of over 40 % in some high latitude regions relative to a comparably low baseline (compare Fig. S5). Similarly, the projected drastic relative reductions of over 60 % for a 2 °C warming in the Amazon region, may not directly affect regional food security, as wheat is not the main regional staple crop (about 1 % of global wheat are produced in the region).

5.2.2 Maize

The effects of elevated CO₂ concentrations affect maize yields to a much lesser extent, as conditions are mostly saturated at present levels (see e.g. Leakey et al., 2006). Differences between runs are thus less pronounced for maize yields, where yield reductions are projected for both the CO₂ and the noCO₂-ensemble. As the number of runs differ between the two ensembles (see Sect. 2), the small differences are likely due to the different ensemble size. Thus, we only discuss results for the CO₂-ensemble here. Differences between the warming levels are significant (all ensemble members indicate a significant difference for the global crop area, see Table S6), with median local yield reductions experienced by 50 % of the global crop area of around 1.5 and 6 % for 1.5 °C and 2 °C warming, respectively. Risks of reductions of up to 26 % at 1.5 °C and 38 % at 2 °C are within the likely range globally (compare Fig. 9 and Table S6).

As apparent in Fig. 9, the likely range is deferred towards stronger reductions. Similar regional patterns compared to wheat projections are apparent. Again, the highest relative median changes occur in regions with a relatively low share of global production. For central North America, where at present about 10 % of global maize is produced, substantial differences between the two warming levels are projected, and

Title Page

Abstract

Introduction

Conclusions

References

Tables

Figures



Back

Close

Full Screen / Esc

Printer-friendly Version

Interactive Discussion



risks for a strong negative effect in this region more than double between 1.5°C and 2°C warming from 15.5 to 37 % (upper limit of the 66 % range). Tropical regions such as Central America, the Amazon and South-East Asia are projected to experience median local yield reductions exceeding 5 % for 1.5°C and up to and more than 10 % for 2°C.

5.2.3 Soy

Projections of changes in soy yields between the two assessed warming levels show robust differences (see Table S7). For the CO₂-ensemble, a median increase in global yields of 7 % is projected for 50 % of the global area under a warming of 1.5°C. This median increase vanishes for 2°C. Global differences between warming levels for the noCO₂-ensemble are smaller but nonetheless robust, with median reductions of 10 and 12 %, respectively.

Regionally, the differences for the noCO₂-ensemble are more pronounced, especially in those regions with a large share in present-day global soy production. Median yields for the Amazon (AMZ) region, currently producing about 7 % of global soy (Monfreda et al., 2008, see also Fig. S5), are projected to reduce from 15 % under 1.5°C to 20 % under 2°C warming. Similar robust differences in yield reductions between 1.5°C and 2°C warming are also projected for the major soy producers in Central North America and South-East South America. For North Asia, where currently over 7 % of soy production takes place, median increases in yields of 28 and 24 % are projected for a warming of 1.5°C for the noCO₂ and CO₂-ensembles, respectively. However, uncertainties for this region are high and a risk of substantial reductions of 25 % (1.5°C) and 20 % (2°C) in the CO₂-ensemble are within the likely range of the ensemble projections.

5.2.4 Rice

Median changes in global rice yields for the CO₂-ensemble do not differ between the assessed warming levels, with projected increases of about 7 % although

Title Page

Abstract

Introduction

Conclusions

References

Tables

Figures



Back

Close

Full Screen / Esc

Printer-friendly Version

Interactive Discussion



Title Page

Abstract

Introduction

Conclusions

References

Tables

Figures



Back

Close

Full Screen / Esc

Printer-friendly Version

Interactive Discussion



the respective local yield change distributions are significantly different (compare Table S8). The distribution of possible developments indicates risks of substantial reductions of up to 17 and 14 % at 1.5°C and 2°C of warming. For the noCO₂-ensemble, reductions of 8 and 15 % are projected for the two warming levels.

The effects of CO₂-fertilization consistently indicates yield increases across regions for median projections. While differences between warming levels are apparent for some regions and the CO₂-ensemble, these display comparably low confidence levels. For the noCO₂-ensemble, robust differences between 1.5°C and 2°C warming are apparent for all major rice producing regions, including all Asian regions where a total of 40 % of rice is produced today (EAS, SAS, SEA, TIB) as well as the Amazon, and South American rice producers. Reductions are projected to double between the two warming levels, for example in South Asia, South-East South America and the Tibetan Plateau. For these regions, median projections are close to the lower end of the likely range (compare Fig. 12 and Table S8).

5.3 Discussion of agricultural impact projections

Our projections of local agricultural yields reveal substantial uncertainties in global median regional yield changes (Figs. 9 to 12) with a likely range (66 % – likelihood) comprising zero. For wheat, rice and soy, our projections indicate differences between the CO₂ and noCO₂ assessments, which are generally much larger than those between a 1.5°C and 2°C warming. While substantial uncertainty renders a differentiation between impacts at 1.5°C and 2°C warming difficult in most world regions, a clear signal emerges for the noCO₂-ensemble, that may serve as a high-risk illustration of potential climate impacts on agricultural production. In the noCO₂-ensemble, local yields are projected to decrease between 1.5°C and 2°C for all crop types.

Our results indicate that risks are region and crop specific and are in line with findings of previous model intercomparison studies (Asseng et al., 2014; Rosenzweig et al., 2013). While high-latitude regions may benefit, median projections for local yields in large parts of the tropical land area are found to be negatively affected

Title Page

Abstract

Introduction

Conclusions

References

Tables

Figures



Back

Close

Full Screen / Esc

Printer-friendly Version

Interactive Discussion



already at 1.5 °C and risks increase substantially, if effects of CO₂-fertilization are less substantial or counter-acted by other factors such as extreme temperature response, land degradation or nitrogen limitation (Rosenzweig et al., 2013; Bodirsky and Müller, 2014; Bodirsky et al., 2014). In a statistical analysis of climate impacts on wheat and barley yields in Europe, Moore and Lobell (2015) report an overall negative contribution of climatic factors in line with findings of a meta-analysis by Asseng et al. (2014), which questions the positive effects projected in our CO₂-ensemble for this region and further support the risk framework of assessing future projections including noCO₂-ensemble projections adopted here. Given that a 1.5 °C warming might be reached already around 2030, our findings underscore the risks of global crop yield reductions due to climate impacts outlined by Lobell and Tebaldi (2014), while giving further indications for the regional diversity of climate impacts with tropical regions being a hot-spot for climate impacts on local agricultural yields (Müller et al., 2014).

6 Sea-level rise

6.1 Methods

Projections for sea-level rise (SLR) cannot be based on a time-sliced approach due to the importance of time-lagged response of ocean and cryosphere to the warming signal. Therefore, we selected two multi-gas scenarios illustrative of a 1.5 °C and 2 °C warming to assess SLR impacts over the the entire 21st century from a large emission scenario ensemble created by Rogelj et al. (2013). These scenarios were created with the integrated assessment modeling framework MESSAGE (the Model for Energy Supply Strategy Alternatives and their General Environmental Impact, Riahi et al., 2007). For both scenarios, temperature projections are derived with the reduced complexity carbon-cycle and climate model MAGICC (Meinshausen et al., 2011) in a probabilistic setup (Meinshausen et al., 2009), which is consistent with the IPCC AR5 assessment of climate sensitivity (Rogelj et al., 2012, 2014). The first scenario

Climate impacts at 1.5 °C and 2 °C

C.-F. Schleussner et al.

Title Page

Abstract

Introduction

Conclusions

References

Tables

Figures



Back

Close

Full Screen / Esc

Printer-friendly Version

Interactive Discussion



keeps GMT to below 2 °C relative to pre-industrial levels (1850–1875) during the 21st century with 50% probability. The second scenario reduces emissions sooner and deeper, and keeps warming to below 1.5 °C relative to pre-industrial levels during the 21st century with about 50% probability and returns end-of-century warming to below 1.5 °C with about 70% probability. See Fig. 13 (upper panel) for median temperature projections for the 2 and 1.5 °C scenario and their associated uncertainty bands. Since the projections for coral reef degradation include a time dependent adaptation scenario, the same approach is taken for the coral reef projections (see Sect. 7).

SLR projections are based on Perrette et al. (2013), who developed a scaling approach for the various SLR contributions according to an appropriately chosen climate predictor – in this case GMT increase and ocean heat uptake. Coupled with output from the MAGICC model, this allows to emulate the sea-level response of GCMs to any kind of emission scenario within the calibration range of the method that is spanned by the RCPs.

Consistent with the relationship found in CMIP3 and CMIP5 GCMs, ocean thermal expansion is assumed to be proportional to cumulative ocean heat uptake (Church et al., 2013). Mountain glacier melt is computed following a widely-used semi-empirical relationship between rate of glacier melt, remaining surface glacier area, and temperature anomaly with respect to pre-industrial levels. This approach assumes constant scaling between area and volume (Wigley and Raper, 2005; Meehl et al., 2007), with parameters chosen to account for current melt rate and known glacier volume (Eq. 1 and Table 2 in Perrette et al., 2013). As already noticed by Gregory and Huybrechts (2006) (their Fig. 5), the surface mass balance (SMB) anomaly from the Greenland ice-sheet can be approximated with reasonable accuracy as a quadratic fit to global mean temperature anomaly. Here we adopted the same functional form, but calibrated it to more recent projections by Fettweis et al. (2013). Following Hinkel et al. (2014), we scaled up these projections by $20 \pm 20\%$ to account for missing dynamic processes (elevation feedback $10 \pm 5\%$, changes in ice dynamics $10 \pm 5\%$, and $\pm 10\%$ arising from the skill of the SMB model to simulate the current SMB rate

over Greenland). The climate-independent land-water contribution has been added for all scenarios following Wada et al. (2012).

Beyond the scaling approach, the real advancement of our approach compared to the IPCC AR5 (Church et al., 2013) stems from the inclusion of scenario-dependent Antarctic ice-sheet projections following Levermann et al. (2014). Linear response functions were derived from idealized step-forcing experiments from the SeaRISE project (Bindschadler et al., 2013) as a functional link between the rate of ice shelf melting and dynamical contribution to SLR over four Antarctic sectors and various ice-sheet models. Levermann et al. (2014) further assume linear scaling between global surface air warming, local ocean warming, and ice-shelf melting in each of the sectors. They adopted a Monte Carlo approach with 50 000 samples to combine the various parameter ranges, GCMs and ice-sheet models. To our knowledge, this is the most comprehensive attempt to date to link climate warming and Antarctic ice-sheet contributions to scenario-dependent sea-level rise over the 21st century.

6.2 Results

The results for the 2°C scenario are comparable with projections by Church et al. (2013) and Hinkel et al. (2014) for RCP2.6 (their Tables 13.5 and 4, respectively) that leads to a median GMT increase of about 1.6°C above pre-industrial levels. For this scenario, we project a median SLR of about 50 cm (36–65 cm, likely range) by 2100 and a rate of rise of 5.6 (4–7) mm year⁻¹ over the 2081–2100 period. Under our illustrative 1.5°C scenario, projected SLR in 2100 is about 20% (or 10 cm) lower, compared to the 2°C scenario (see Table 2). The corresponding reduction in the expected rate of SLR over the 2081–2100 period is about 30%. More importantly, and in contrast to the projections for the 2°C scenario, the rate for the 1.5°C scenario is projected to decline between mid-century and the 2081–2100 period by about 0.5 mm year⁻¹, which substantially reduces the multi-centennial SLR commitment (Schaeffer et al., 2012).

The projected difference in SLR between the 1.5°C and 2°C scenarios studied here is comparable to the difference between the RCP2.6 and RCP4.5 scenarios (Hinkel

Title Page

Abstract

Introduction

Conclusions

References

Tables

Figures



Back

Close

Full Screen / Esc

Printer-friendly Version

Interactive Discussion



Climate impacts at 1.5 °C and 2 °C

C.-F. Schleussner et al.

Title Page

Abstract

Introduction

Conclusions

References

Tables

Figures



Back

Close

Full Screen / Esc

Printer-friendly Version

Interactive Discussion



et al., 2014; Church et al., 2013), while the projected median GMT difference between the two RCP scenarios is about 0.8 °C for the 2081–2100 period. The relatively higher sensitivity of SLR in the 21st century to temperature increase at low climate warming is probably related to the earlier peaking of GMT under such scenarios and thus an already longer adjustment period for the time-lagged ocean and cryosphere. This leads to a larger share of committed multi-centennial SLR to occur in the 21st century. On multi-centennial timescales these scenario dependent differences are expected to vanish. A long-term difference, however, may arise from contributions by mountain glacier melt, which are particularly vulnerable to GMT increase and thus differences in melted mountain glacier volume are higher for lower emission scenarios.

While SLR projections for the two illustrative 1.5 °C and 2 °C differ substantially, this effect is strongly scenario dependent. In particular, most emission pathways labeled as 1.5 °C scenarios allow for a temporal overshoot in GMT and a decline below 1.5 °C with a 50 % probability by 2100 (Rogelj et al., 2015), whereas the illustrative 1.5 °C scenario used here does not allow for a GMT overshoot, but stays below 1.5 °C over the course of the 21st century. For time-lagged climate impacts such as SLR that depend on the cumulative heat entry in the system, the difference between a scenario allowing for a GMT overshoot and one that does not will be significant.

Sea-level adjustment to climate warming has a time scale much larger than a century as a result of slow ice-sheet processes and ocean heat uptake. This means that in all emission scenarios considered, sea level will continue to rise beyond 2100. Levermann et al. (2013) have shown that on a 2000 year time-scale, sea-level sensitivity to global mean temperature increase is about 2.3 m per °C. In addition to that, Levermann et al. (2013) report a steep increase in long-term SLR between 1.5 °C and 2 °C as a result of an increasing risk of crossing a destabilizing threshold for the Greenland ice-sheet (Robinson et al., 2012). The disintegration of this ice-sheet, which would lead to 5–7 m global SLR, is projected to happen on the time scale of several millennia, however.

Recent observational and modeling evidence indicates that a marine ice-sheet instability in the West Antarctic may have already been triggered, which could lead

to an additional SLR commitment of about 1 m on a multi-centennial time scale. Spillover effects of this destabilization on other drainage basins and their relation to GMT increase are as yet little understood (Rignot et al., 2014; Joughin et al., 2014; Favier et al., 2014). Similarly, Mengel and Levermann (2014) report a potential marine ice-sheet instability for the Wilkens Basin in West Antarctica containing 3–4 m of global SLR. The dynamics of these coupled cryosphere-oceanic systems remain a topic of intense research. Current fine-scale ocean models, suggest increased intrusion of warm deep water on the continental shelf as a result of anthropogenic climate change and thus indicate an increasing risk with increasing warming (Hellmer et al., 2012; Timmermann and Hellmer, 2013). Given the risk of potentially triggering multi-meter SLR on centennial to millennial time scales, this clearly calls for a precautionary approach that is further underscored by evidence from paleo-records, which reveals that past sea-levels might have about 6–9 m above present day for levels for a GMT increase not exceeding 2 °C above pre-industrial levels (Dutton et al., 2015).

7 Coral reef systems

7.1 Methods

The projections of the degradation of coral reef sites use a risk assessment framework analogous to the coral bleaching model developed in Frieler et al. (2012) based on the two illustrative 1.5 °C and 2 °C global emission pathways introduced in Sect. 6.1. The framework applies a threshold-based bleaching algorithm by Donner (2009), which is based on degree heating months (DHMs), to sea surface temperature (SST) pathways of 2160 individual geospatial locations of coral reef sites (see www.reefbase.org) and generates as output the fraction of coral reef locations subject to long-term degradation. DHMs are a measure for the accumulated heat stress exerted on coral reefs due to elevated SST (see Fig. S6 for a graphical illustration of the methodology). Within a four months moving window the monthly SST above a reference value (here the mean of

[Title Page](#)
[Abstract](#)
[Introduction](#)
[Conclusions](#)
[References](#)
[Tables](#)
[Figures](#)
[Back](#)
[Close](#)
[Full Screen / Esc](#)
[Printer-friendly Version](#)
[Interactive Discussion](#)


Climate impacts at 1.5 °C and 2 °C

C.-F. Schleussner et al.

Title Page

Abstract

Introduction

Conclusions

References

Tables

Figures



Back

Close

Full Screen / Esc

Printer-friendly Version

Interactive Discussion



monthly maximal temperatures, MMM) are accumulated and compared to a threshold value (critical DHM threshold) that is associated with mass coral bleaching. The value of the critical DHM threshold depends on the scenario assumptions (see below). In order to translate coral bleaching events into long-term coral degradation, we refer to the assumption that reef recovery from mass coral bleaching is usually very limited within the first five years (Baker et al., 2008). Therefore, we assume a maximum tolerable probabilistic frequency of 0.2 year^{-1} (Donner, 2009) for bleaching events causing long-term degradation. The MMM is calculated from a 20 year climatological reference period (1980–2000) individually for every coral location and SST pathway. Thus, the MMM serves as an indicator of temperatures to which the corals of a certain reef location are generally adapted. In order to generate a scenario-independent description of coral reef response to different levels of global warming (e.g. any given global mean air temperature pathway) we apply the algorithm to a large number of SST pathways and reassign the fraction of 2160 mapped coral reef locations subject to long-term degradation back to global air temperature pathways. In total, we use the SST pathways of 19 Atmosphere–Ocean General Circulation Models (AOGCMs) from the multi-model CMIP3 project and seven different emission scenarios leading to 30 728 model years. We also used a wide range of critical DHMs (from 0 to 8°), which allows for the testing of risk scenarios with constant and variable critical DHM thresholds (e.g. thermal adaptation).

The condensed output of the global coral bleaching assessment allows for the implementation of different coral adaptation scenarios. In the standard scenario (Constant) a constant DHM threshold of 2 °C is assumed. This means that corals can resist a cumulative heat stress of 2 °C (accumulated over four month period) above the long-term maximum monthly mean (MMM) sea surface temperature for a given location. It has been demonstrated that this value serves as a good proxy for severe mass coral bleaching (Donner et al., 2005, 2007).

In addition to the constant scenario, an extremely optimistic scenario of strong thermal adaptation of the corals is assessed (Adaptation). Under this scenarios,

reduced to about 70 % of global coral reef cells under a 1.5°C scenario but not under a 2°C scenario (compare Fig. 14 and Table 3).

Our approach only includes the effects of increased CO₂-concentrations, but does not account for other stressors for coral reef systems such as rising sea-levels, increased intensity of ENSO-events (Power et al., 2013), tropical cyclones (Knutson et al., 2010), invasive species and disease spreading (Maynard et al., 2015), and other local anthropogenic stressors, which ranks our projections of long-term coral reef degradation rather conservative. These projected losses will greatly affect societies, which depend on coral reefs as a primary source of ecosystem services e.g. in the fishery and tourism sector (Cinner et al., 2015). Teh et al. (2013) estimate that about 25 % of the world's small-scale fishers fish on coral reefs. Chen et al. (2015) report that a loss of less than 60 % of global coral reef coverage, that could very well be reached already in the 2030s, would inflict damages of more than USD 20 billion annually.

8 Discussion and conclusions

The findings of our analysis support the IPCC RFC assessment of differences in key impacts of climate change between warming of 1.5°C and 2°C above pre-industrial levels: we find that under a 1.5° scenario, the fractions of coral reef cells under risk of severe degradation are reduced significantly compared to a warming of 2°C (RFC1), that the difference between 1.5°C and 2°C marks the transition between an upper limit of present-day natural variability and a new climate regime in terms of heat extremes globally (RFC2), and that changes in water availability and local agricultural yields are already unevenly distributed between world regions at 1.5°C and even more so at 2°C (RFC3).

Water availability reduction and dry spell length (CDD) increase are found to accelerate between 1.5°C and 2°C for several sub-tropical regions, in particular in the Mediterranean, Central America and the Caribbean, South Africa and Australia. Local agriculture production in tropical regions is projected to be strongly affected by ongoing

Title Page

Abstract

Introduction

Conclusions

References

Tables

Figures



Back

Close

Full Screen / Esc

Printer-friendly Version

Interactive Discussion



warming, in particular, if effects of CO₂-fertilization do not play out as current models project them or are counter-balanced by other factors such as nitrogen and phosphorus limitations or heat stress, which are not fully included in the models investigated here.

Our analysis of projected SLR reveals differences of about 10 cm in global mean SLR between a illustrative 1.5°C and 2°C scenario by 2100. In addition, recent findings outlining evidence from the paleo-record (Dutton et al., 2015) and modeling studies (Levermann et al., 2013) indicate that a multi-meter sea-level of potentially up to 9 m and is not unlikely under a 2°C warming on multi-millennial time scales. In particular, a maintained warming of 2°C above pre-industrial levels has been found to potentially destabilize large parts of the Greenland ice-sheet (Robinson et al., 2012) and a warming of well-below 2°C might be needed to avoid further destabilization of marine ice-sheets in Antarctica (Winkelmann et al., 2015). We are only beginning to understand the complex ocean–ice-sheet interactions that govern these processes and as a consequence, these thresholds are subject to substantial uncertainty and call for a precautionary approach to keep warming as low as possible.

Our assessment based on this limited set of indicators implies that differences in climate impacts between 1.5°C and 2°C are most pronounced for particularly vulnerable regions and for groups in countries with limited adaptive capacity (Olsson et al., 2014). Under a 2°C warming, coastal tropical regions and islands may face the combined effects of a near-complete loss of tropical coral reefs, which provide coastal protection and are a main source of ecosystem services, on-going sea-level rise above present day rates over the 21st century and increased threats by coastal flooding and inundation. The risks posed by extreme heat and potential crop yield reductions in tropical regions in Africa and South East Asia under a 2°C warming are particularly critical given the projected trends in population growth and urbanization in these regions (O’Neill et al., 2013). In conjunction with other development challenges, the impacts of climate change represent a fundamental challenge for regional food security (Lobell and Tebaldi, 2014) and may trigger new poverty traps for several countries or populations within countries (Olsson et al., 2014).

Title Page

Abstract

Introduction

Conclusions

References

Tables

Figures



Back

Close

Full Screen / Esc

Printer-friendly Version

Interactive Discussion



**Climate impacts at
1.5 °C and 2 °C**

C.-F. Schleussner et al.

Title Page

Abstract

Introduction

Conclusions

References

Tables

Figures

I◀

▶I

◀

▶

Back

Close

Full Screen / Esc

Printer-friendly Version

Interactive Discussion



Furthermore, the emergence of the Mediterranean region, including North Africa and the Levant, as a hot-spot for reductions in water availability and dry spell increases between 1.5 °C and 2 °C is of great relevance given the specific vulnerability of this region to water scarcity (Schellnhuber et al., 2014). The political instability in several countries in this region may further exacerbate the vulnerability of societies to climatic stresses, potentially increasing the risk of violent conflict outbreak (Kelley et al., 2015).

In conjunction with a recent analysis of requirements and costs of energy system transformation pathways in line with limiting warming to below 1.5 °C in 2100 (Rogelj et al., 2015), we hope that our analysis can contribute to inform the discussion about the adequacy of different long-term climate targets. In the light of the upcoming UNFCCC negotiations in Paris in December 2015, where a global agreement on limit climate change is anticipated, a comprehensive overview of the consequences of different temperature-pathways is essential to reach informed decisions.

**The Supplement related to this article is available online at
doi:10.5194/esdd-6-2447-2015-supplement.**

Acknowledgements. We acknowledge the World Climate Research Programme's Working Group on Coupled Modelling, which is responsible for CMIP, and we thank the climate modeling groups for producing and making available their model output. For CMIP, the US Department of Energy's Program for Climate Model Diagnosis and Intercomparison provided coordinating support and led development of software infrastructure in partnership with the Global Organization for Earth System Science Portals. We would like to thank the modelling groups that participated in the Inter-Sectoral Impact Model Intercomparison Project (ISI-MIP).

The ISI-MIP Fast Track project underlying this paper was funded by the German Federal Ministry of Education and Research with project funding reference number 01LS1201A. The work on this paper was supported by the Federal Ministry for the Environment, Nature Conservation and Nuclear Safety (11II093 Global A SIDS and LDCs).

References

- Asseng, S., Ewert, F., Martre, P., Rötter, R., Lobell, D., Cammarano, D., Kimball, B. a., Ottman, M., Wall, G., White, J., Reynolds, M., Alderman, P., Prasad, P., Aggarwal, P., Anothai, J., Basso, B., Biernath, C., Challinor, A., De Sanctis, G., Doltra, J., Fereres, E., Garcia-Vila, M., Gayler, S., Hoogenboom, G., Hunt, L., Izaurrealde, R., Jabloun, M., Jones, C., Kersebaum, K., Koehler, A.-K., Müller, C., Naresh Kumar, S., Nendel, C., O'Leary, G., Olesen, J., Palosuo, T., Priesack, E., Eyshi Rezaei, E., Ruane, A., Semenov, M., Shcherbak, I., Stöckle, C., Stratonovitch, P., Streck, T., Supit, I., Tao, F., Thorburn, P., Waha, K., Wang, E., Wallach, D., Wolf, J., Zhao, Z., and Zhu, Y.: Rising temperatures reduce global wheat production, *Nature Climate Change*, 5, 143–147, doi:10.1038/nclimate2470, 2014. 2465, 2466
- Ault, T. R., Cole, J. E., Overpeck, J. T., Pederson, G. T., and Meko, D. M.: Assessing the risk of persistent drought using climate model simulations and paleoclimate data, *J. Climate*, 27, 7529–7549, doi:10.1175/JCLI-D-12-00282.1, 2014. 2459
- Baker, A. C., Glynn, P. W., and Riegl, B.: Climate change and coral reef bleaching: an ecological assessment of long-term impacts, recovery trends and future outlook, *Estuar. Coast. Shelf S.*, 80, 435–471, doi:10.1016/j.ecss.2008.09.003, 2008. 2471
- Bindschadler, R. A., Nowicki, S., Abe-OUCHI, A., Aschwanden, A., Choi, H., Fastook, J., Granzow, G., Greve, R., Gutowski, G., Herzfeld, U., Jackson, C., Johnson, J., Khroulev, C., Levermann, A., Lipscomb, W. H., Martin, M. a., Morlighem, M., Parizek, B. R., Pollard, D., Price, S. F., Ren, D., Saito, F., Sato, T., Seddik, H., Seroussi, H., Takahashi, K., Walker, R., and Wang, W. L.: Ice-sheet model sensitivities to environmental forcing and their use in projecting future sea level (the SeaRISE project), *J. Glaciol.*, 59, 195–224, doi:10.3189/2013JoG12J125, 2013. 2468
- Bodirsky, B. L. and Müller, C.: Robust relationship between yields and nitrogen inputs indicates three ways to reduce nitrogen pollution, *Environ. Res. Lett.*, 9, 111005, doi:10.1088/1748-9326/9/11/111005, 2014. 2466
- Bodirsky, B. L., Popp, A., Lotze-Campen, H., Dietrich, J. P., Rolinski, S., Weindl, I., Schmitz, C., Müller, C., Bonsch, M., Humpenöder, F., Biewald, A., and Stevanovic, M.: Reactive nitrogen requirements to feed the world in 2050 and potential to mitigate nitrogen pollution, *Nature Communications*, 5, 3858, doi:10.1038/ncomms4858, 2014. 2466

ESDD

6, 2447–2505, 2015

Climate impacts at
1.5 °C and 2 °C

C.-F. Schleussner et al.

Title Page

Abstract

Introduction

Conclusions

References

Tables

Figures

◀

▶

◀

▶

Back

Close

Full Screen / Esc

Printer-friendly Version

Interactive Discussion



Climate impacts at 1.5 °C and 2 °C

C.-F. Schleussner et al.

Title Page

Abstract

Introduction

Conclusions

References

Tables

Figures



Back

Close

Full Screen / Esc

Printer-friendly Version

Interactive Discussion



Boers, N., Bookhagen, B., Barbosa, H., Marwan, N., and Kurths, J.: Prediction of extreme floods in the Central Andes by means of complex networks, *Nature Communications*, 16, 7173, doi:10.1038/ncomms6199, 2014. 2458

Caldeira, K.: Ocean model predictions of chemistry changes from carbon dioxide emissions to the atmosphere and ocean, *J. Geophys. Res.*, 110, 1–12, doi:10.1029/2004JC002671, 2005. 2472

Chen, P.-Y., Chen, C.-C., Chu, L., and Mccarl, B.: Evaluating the economic damage of climate change on global coral reefs, *Global Environ. Chang.*, 30, 12–20, doi:10.1016/j.gloenvcha.2014.10.011, 2015. 2473

Church, J. A., Clark, P. U., Cazenave, A., Gregory, J. M., Jevrejeva, S., Levermann, A., Merrifield, M. A., Milne, G. A., Nerem, R. S., Nunn, P. D., Payne, A. J., Pfeffer, W. T., Stammer, D., and Unnikrishnan, A. S.: Sea Level Change, in: *Climate Change 2013: The Physical Science Basis. Contribution of Working Group I to the Fifth Assessment Report of the Intergovernmental Panel on Climate Change*, edited by: Stocker, T. F., Qin, D., Plattner, G.-K., Tignor, M., Allen, S. K., Boschung, J., Nauels, A., Xia, Y., Bex, V., and Midgley, P. M., Cambridge University Press, Cambridge, United Kingdom and New York, NY, USA, 2013. 2467, 2468, 2469

Cinner, J. E., Pratchett, M. S., Graham, N. A. J., Messmer, V., Fuentes, M. M. P. B., Ainsworth, T., Ban, N., Bay, L. K., Blythe, J., Disard, D., Dunn, S., Evans, L., Fabinyi, M., Fidelman, P., Figueiredo, J., Frisch, A. J., Fulton, C. J., Hicks, C. C., Lukoschek, V., Mallela, J., Moya, A., Penin, L., Rummer, J. L., Walker, S., and Williamson, D. H.: A framework for understanding climate change impacts on coral reef social–ecological systems, *Reg. Environ. Change*, doi:10.1007/s10113-015-0832-z, online first, 2015. 2473

Coumou, D. and Robinson, A.: Historic and future increase in the global land area affected by monthly heat extremes, *Environ. Res. Lett.*, 8, 034018, doi:10.1088/1748-9326/8/3/034018, 2013. 2457

Dai, A.: Increasing drought under global warming in observations and models, *Nature Climate Change*, 3, 52–58, doi:10.1038/nclimate1633, 2012. 2459

Deryng, D., Conway, D., Ramankutty, N., Price, J., and Warren, R.: Global crop yield response to extreme heat stress under multiple climate change futures, *Environ. Res. Lett.*, 9, 034011, doi:10.1088/1748-9326/9/3/034011, 2014. 2457, 2461

Title Page

Abstract

Introduction

Conclusions

References

Tables

Figures

◀

▶

◀

▶

Back

Close

Full Screen / Esc

Printer-friendly Version

Interactive Discussion



- Diffenbaugh, N. S. and Scherer, M.: Observational and model evidence of global emergence of permanent, unprecedented heat in the 20th and 21st centuries, *Climatic Change*, 107, 615–624, doi:10.1007/s10584-011-0112-y, 2011. 2457
- Donner, S. D.: Coping with commitment: projected thermal stress on coral reefs under different future scenarios, *PLoS one*, 4, e5712, doi:10.1371/journal.pone.0005712, 2009. 2470, 2471
- Donner, S. D., Skirving, W. J., Little, C. M., Oppenheimer, M., and Hoegh-Gulberg, O.: Global assessment of coral bleaching and required rates of adaptation under climate change, *Glob. Change Biol.*, 11, 2251–2265, doi:10.1111/j.1365-2486.2005.01073.x, 2005. 2471
- Donner, S. D., Knutson, T. R., and Oppenheimer, M.: Model-based assessment of the role of human-induced climate change in the 2005 Caribbean coral bleaching event., *P. Natl. Acad. Sci. USA*, 104, 5483–5488, doi:10.1073/pnas.0610122104, 2007. 2471
- Dutton, A., Carlson, A. E., Long, A. J., Milne, G. A., Clark, P. U., DeConto, R., Horton, B. P., Rahmstorf, S., and Raymo, M. E.: Sea-level rise due to polar ice-sheet mass loss during past warm periods, *Science*, 349, 6244, doi:10.1126/science.aaa4019, 2015. 2470, 2474
- Eamus, D.: The interaction of rising CO₂ and temperatures with water use efficiency, *Plant Cell Environ.*, 14, 843–852, doi:10.1111/j.1365-3040.1991.tb01447.x, 1991. 2461
- Favier, L., Durand, G., Cornford, S. L., Gudmundsson, G. H., Gagliardini, O., Gillet-Chaulet, F., Zwinger, T., Payne, A. J., and Le Brocq, A. M.: Retreat of Pine Island Glacier controlled by marine ice-sheet instability, *Nature Climate Change*, 4, 117–121, doi:10.1038/nclimate2094, 2014. 2470
- Fettweis, X., Franco, B., Tedesco, M., van Angelen, J. H., Lenaerts, J. T. M., van den Broeke, M. R., and Gallée, H.: Estimating the Greenland ice sheet surface mass balance contribution to future sea level rise using the regional atmospheric climate model MAR, *The Cryosphere*, 7, 469–489, doi:10.5194/tc-7-469-2013, 2013. 2467
- Fischer, E. and Knutti, R.: Detection of spatially aggregated changes in temperature and precipitation extremes, *Geophys. Res. Lett.*, 41, 547–554, doi:10.1002/2013GL058499, 2014. 2453
- Fischer, E. M., Beyerle, U., and Knutti, R.: Robust spatially aggregated projections of climate extremes, *Nature Climate Change*, 3, 1033–1038, doi:10.1038/nclimate2051, 2013. 2453, 2454
- Flato, G., Marotzke, J., Abiodun, B., Braconnot, P., Chou, S. C., Collins, W., Cox, P., Driouech, F., Emori, S., Eyring, V., Forest, C., Gleckler, P., Guilyardi, E., Jakob, C., Kattsov, V., Reason, C., and Rummukainen, M.: Evaluation of climate models, in: *Climate Change 2013: The Physical*

**Climate impacts at
1.5 °C and 2 °C**

 C.-F. Schleussner et al.

[Title Page](#)
[Abstract](#)
[Introduction](#)
[Conclusions](#)
[References](#)
[Tables](#)
[Figures](#)

[Back](#)
[Close](#)
[Full Screen / Esc](#)
[Printer-friendly Version](#)
[Interactive Discussion](#)


Science Basis. Contribution of Working Group I to the Fifth Assessment Report of the Intergovernmental Panel on Climate, Cambridge University Press, Cambridge, UK, New York, NY, USA, 741–866, doi:10.1017/CBO9781107415324.020, 2013. 2452

5 Frieler, K., Meinshausen, M., Golly, A., Mengel, M., Lebek, K., Donner, S. D., and Hoegh-Guldberg, O.: Limiting global warming to 2 °C is unlikely to save most coral reefs, *Nature Climate Change*, 3, 165–170, doi:10.1038/nclimate1674, 2012. 2470, 2472, 2505

10 Frieler, K., Levermann, A., Elliott, J., Heinke, J., Arneth, A., Bierkens, M. F. P., Ciais, P., Clark, D. B., Deryng, D., Döll, P., Falloon, P., Fekete, B., Folberth, C., Friend, A. D., Gellhorn, C., Gosling, S. N., Haddeland, I., Khabarov, N., Lomas, M., Masaki, Y., Nishina, K., Neumann, K., Oki, T., Pavlick, R., Ruane, A. C., Schmid, E., Schmitz, C., Stacke, T., Stehfest, E., Tang, Q., Wisser, D., Huber, V., Piontek, F., Warszawski, L., Schewe, J., Lotze-Campen, H., and Schellnhuber, H. J.: A framework for the cross-sectoral integration of multi-model impact projections: land use decisions under climate impacts uncertainties, *Earth Syst. Dynam.*, 6, 447–460, doi:10.5194/esd-6-447-2015, 2015. 2451

15 Gattuso, J.-P., Magnan, A., Bille, R., Cheung, W. W. L., Howes, E. L., Joos, F., Allemand, D., Bopp, L., Cooley, S. R., Eakin, C. M., Hoegh-Guldberg, O., Kelly, R. P., Portner, H.-O., Rogers, A. D., Baxter, J. M., Laffoley, D., Osborn, D., Rankovic, A., Rochette, J., Sumaila, U. R., and Treyer, S.: Contrasting futures for ocean and society from different anthropogenic CO₂ emissions scenarios, *Science*, 349, 6243, doi:10.1126/science.aac4722, 2015. 2472

20 Gourdji, S. M., Sibley, A. M., and Lobell, D. B.: Global crop exposure to critical high temperatures in the reproductive period: historical trends and future projections, *Environ. Res. Lett.*, 8, 024041, doi:10.1088/1748-9326/8/2/024041, 2013. 2461

25 Graham, N. A. J., Jennings, S., Macneil, M. A., Mouillot, D., and Wilson, S. K.: Predicting climate-driven regime shifts versus rebound potential in coral reefs, *Nature*, 518, 94–97, doi:10.1038/nature14140, 2015. 2472

Gregory, J. M. and Huybrechts, P.: Ice-sheet contributions to future sea-level change, *Philos. T. R. Soc. A*, 364, 1709–1732, doi:10.1098/rsta.2006.1796, 2006. 2467

30 Hansen, J., Sato, M., and Ruedy, R.: Perception of climate change, *P. Natl. Acad. Sci. USA*, 107, E2415–E2423, doi:10.1073/pnas.1205276109, 2012. 2457

Hellmer, H. H., Kauker, F., Timmermann, R., Determann, J., and Rae, J.: Twenty-first-century warming of a large Antarctic ice-shelf cavity by a redirected coastal current, *Nature*, 485, 225–228, doi:10.1038/nature11064, 2012. 2470

**Climate impacts at
1.5 °C and 2 °C**

 C.-F. Schleussner et al.

[Title Page](#)
[Abstract](#)
[Introduction](#)
[Conclusions](#)
[References](#)
[Tables](#)
[Figures](#)

[Back](#)
[Close](#)
[Full Screen / Esc](#)
[Printer-friendly Version](#)
[Interactive Discussion](#)


Hempel, S., Frieler, K., Warszawski, L., Schewe, J., and Piontek, F.: A trend-preserving bias correction – the ISI-MIP approach, *Earth Syst. Dynam.*, 4, 219–236, doi:10.5194/esd-4-219-2013, 2013. 2459

Hinkel, J., Lincke, D., Vafeidis, A. T., Perrette, M., Nicholls, R. J., Tol, R. S. J., Marzeion, B., Fettweis, X., Ionescu, C., and Levermann, A.: Coastal flood damage and adaptation costs under 21st century sea-level rise, *P. Natl. Acad. Sci. USA*, 111, 3292–3297, doi:10.1073/pnas.1222469111, 2014. 2467, 2468

Hirabayashi, Y., Mahendran, R., Koirala, S., Konoshima, L., Yamazaki, D., Watanabe, S., Kim, H., and Kanae, S.: Global flood risk under climate change, *Nature Climate Change*, 3, 1–6, doi:10.1038/nclimate1911, 2013. 2459

IPCC: Managing the Risks of Extreme Events and Disasters to Advance Climate Change Adaptation (SREX), Cambridge University Press, Cambridge, doi:10.1017/CBO9781139177245, 2012. 2453, 2454, 2458, 2489

IPCC: Summary for policymakers, in: *Climate Change 2013: The Physical Science Basis. Contribution of Working Group I to the Fifth Assessment Report of the Intergovernmental Panel on Climate Change*, edited by: Stocker, T., Qin, D., Plattner, G.-K., Tignor, M., Allen, S., Boschung, J., Nauels, A., Xia, Y., Bex, V., and Midgley, P., IPCC AR5 WGI, Cambridge University Press, Cambridge, UK, New York, NY, USA, 1–100, 2013. 2449, 2450, 2452, 2454

IPCC: *Climate Change 2014: Synthesis Report. Contribution of Working Groups I, II and III to the Fifth Assessment Report of the Intergovernmental Panel on Climate Change*, IPCC, Geneva, Switzerland, 151 pp., 2014a. 2449, 2450

IPCC: Summary for policy makers, in: *Climate Change 2014: Impacts, Adaptation and Vulnerability – Contributions of the Working Group II to the Fifth Assessment Report*, edited by: Field, C. B., Barros, V. R., Dokken, D., Mach, K. J., Mastrandrea, M. D., Bilir, T. E., Chatterjee, M., Ebi, K. L., Estrada, Y., Genova, R., Girma, B., Kissel, E., Levy, A., MacCracken, S., Mastrandrea, P. R., and White, L., Cambridge University Press, Cambridge, UK, New York, NY, USA, 1–32, doi:10.1016/j.renene.2009.11.012, 2014b. 2454

James, R. and Washington, R.: Changes in African temperature and precipitation associated with degrees of global warming, *Climatic Change*, 117, 859–872, doi:10.1007/s10584-012-0581-7, 2013. 2459

**Climate impacts at
1.5 °C and 2 °C**

 C.-F. Schleussner et al.

[Title Page](#)
[Abstract](#)
[Introduction](#)
[Conclusions](#)
[References](#)
[Tables](#)
[Figures](#)

[Back](#)
[Close](#)
[Full Screen / Esc](#)
[Printer-friendly Version](#)
[Interactive Discussion](#)


Joughin, I., Smith, B. E., and Medley, B.: Marine ice sheet collapse potentially underway for the Thwaites Glacier Basin, West Antarctica, *Science*, 344, 735–388, doi:10.1126/science.1249055, 2014. 2470

5 Kelley, C. P., Mohtadi, S., Cane, M. a., Seager, R., and Kushnir, Y.: Climate change in the Fertile Crescent and implications of the recent Syrian drought, *P. Natl. Acad. Sci. USA*, 112, 3241–3246, doi:10.1073/pnas.1421533112, 2015. 2475

Kendon, E. J., Rowell, D. P., Jones, R. G., and Buonomo, E.: Robustness of future changes in local precipitation extremes, *J. Climate*, 21, 4280–4297, doi:10.1175/2008JCLI2082.1, 2008. 2453

10 Kharin, V. V., Zwiers, F. W., Zhang, X., and Wehner, M.: Changes in temperature and precipitation extremes in the CMIP5 ensemble, *Climatic Change*, 119, 345–357, doi:10.1007/s10584-013-0705-8, 2013. 2457

Kiem, A. S. and Verdon-Kidd, D. C.: Towards understanding hydroclimatic change in Victoria, Australia – preliminary insights into the “Big Dry”, *Hydrol. Earth Syst. Sci.*, 14, 433–445, doi:10.5194/hess-14-433-2010, 2010. 2459

15 King, A. D., Donat, M. G., Fischer, E. M., Hawkins, E., Alexander, L. V., Karoly, D. J., Dittus, A. J., Lewis, S. C., and Perkins, S. E.: The timing of anthropogenic emergence in simulated climate extremes, *Environ. Res. Lett.*, 10, 094015, doi:10.1088/1748-9326/10/9/094015, 2015. 2449, 2454, 2457

20 Knutson, T. R., McBride, J. L., Chan, J., Emanuel, K., Holland, G., Landsea, C., Held, I., Kossin, J. P., Srivastava, A. K., and Sugi, M.: Tropical cyclones and climate change, *Nat. Geosci.*, 3, 157–163, doi:10.1038/ngeo779, 2010. 2473

Knutti, R. and Sedláček, J.: Robustness and uncertainties in the new CMIP5 climate model projections, *Nature Climate Change*, 3, 369–373, doi:10.1038/nclimate1716, 2012. 2452, 2460

25 Leakey, A. D. B., Urbelarrea, M., Ainsworth, E. a., Naidu, S. L., Rogers, A., Ort, D. R., and Long, S. P.: Photosynthesis, productivity, and yield of maize are not affected by open-air elevation of CO₂ concentration in the absence of drought, *Plant Physiol.*, 140, 779–790, doi:10.1104/105 pp.073957, 2006. 2463

30 Levermann, A., Clark, P. U., Marzeion, B., Milne, G. a., Pollard, D., Radic, V., and Robinson, A.: The multimillennial sea-level commitment of global warming, *P. Natl. Acad. Sci. USA*, 110, 13745–13750, doi:10.1073/pnas.1219414110, 2013. 2469, 2474

**Climate impacts at
1.5 °C and 2 °C**

 C.-F. Schleussner et al.

[Title Page](#)
[Abstract](#)
[Introduction](#)
[Conclusions](#)
[References](#)
[Tables](#)
[Figures](#)
[◀](#)
[▶](#)
[◀](#)
[▶](#)
[Back](#)
[Close](#)
[Full Screen / Esc](#)
[Printer-friendly Version](#)
[Interactive Discussion](#)


Levermann, A., Winkelmann, R., Nowicki, S., Fastook, J. L., Frieler, K., Greve, R., Hellmer, H. H., Martin, M. A., Meinshausen, M., Mengel, M., Payne, A. J., Pollard, D., Sato, T., Timmermann, R., Wang, W. L., and Bindschadler, R. A.: Projecting Antarctic ice discharge using response functions from SeaRISE ice-sheet models, *Earth Syst. Dynam.*, 5, 271–293, doi:10.5194/esd-5-271-2014, 2014. 2468

Lobell, D. B. and Tebaldi, C.: Getting caught with our plants down: the risks of a global crop yield slowdown from climate trends in the next two decades, *Environ. Res. Lett.*, 9, 074003, doi:10.1088/1748-9326/9/7/074003, 2014. 2466, 2474

Marotzke, J. and Forster, P. M.: Forcing, feedback and internal variability in global temperature trends, *Nature*, 517, 565–570, doi:10.1038/nature14117, 2014. 2452

Maynard, J., van Hooidonk, R., Eakin, C. M., Puotinen, M., Garren, M., Williams, G., Heron, S. F., Lamb, J., Weil, E., Willis, B., and Harvell, C. D.: Projections of climate conditions that increase coral disease susceptibility and pathogen abundance and virulence, *Nature Climate Change*, 5, 688–694, doi:10.1038/nclimate2625, 2015. 2472, 2473

McGrath, J. M. and Lobell, D. B.: Regional disparities in the CO₂ fertilization effect and implications for crop yields, *Environ. Res. Lett.*, 8, 014054, doi:10.1088/1748-9326/8/1/014054, 2013. 2461

Meehl, G., Stocker, T., Collins, W., Friedlingstein, P., Gaye, A., Gregory, J., Kitoh, A., Knutti, R., Murphy, J., Noda, A., Raper, S., Watterson, I., Weaver, A., and Zhao, Z.-C.: Global climate projections, in: *Climate Change 2007: The Physical Science Basis. Contribution of Working Group I to the Fourth Assessment Report of the Intergovernmental Panel on Climate Change*, edited by: Solomon, S., Qin, D., Manning, M., Chen, Z., Marquis, M., Averyt, K., Tignor, M., and Miller, H., Cambridge University Press, Cambridge, UK, New York, NY, USA, chap. 10, 747–845, 2007. 2467

Meinshausen, M., Meinshausen, N., Hare, W., Raper, S. C. B., Frieler, K., Knutti, R., Frame, D. J., and Allen, M. R.: Greenhouse-gas emission targets for limiting global warming to 2 °C, *Nature*, 458, 1158–1162, doi:10.1038/nature08017, 2009. 2466

Meinshausen, M., Raper, S. C. B., and Wigley, T. M. L.: Emulating coupled atmosphere-ocean and carbon cycle models with a simpler model, *MAGICC6 – Part 1: Model description and calibration*, *Atmos. Chem. Phys.*, 11, 1417–1456, doi:10.5194/acp-11-1417-2011, 2011. 2466

Title Page

Abstract

Introduction

Conclusions

References

Tables

Figures



Back

Close

Full Screen / Esc

Printer-friendly Version

Interactive Discussion



- Meissner, K. J., Lippmann, T., and Sen Gupta, A.: Large-scale stress factors affecting coral reefs: open ocean sea surface temperature and surface seawater aragonite saturation over the next 400 years, *Coral Reefs*, 31, 309–319, doi:10.1007/s00338-011-0866-8, 2012. 2472
- Mengel, M. and Levermann, A.: Ice plug prevents irreversible discharge from East Antarctica, *Nature Climate Change*, 27, 1–5, doi:10.1038/NCLIMATE2226, 2014. 2470
- Monfreda, C., Ramankutty, N., and Foley, J.: Farming the planet: 2. Geographic distribution of crop areas, yields, physiological types, and net primary production in the year 2000, *Global Biogeochem. Cy.*, 22, 1–19, doi:10.1029/2007GB002947, 2008. 2461, 2464, 2500
- Moore, F. C. and Lobell, D. B.: The fingerprint of climate trends on European crop yields, *P. Natl. Acad. Sci. USA*, 112, 2670–2675, doi:10.1073/pnas.1409606112, 2015. 2466
- Mora, C., Frazier, A. G., Longman, R. J., Dacks, R. S., Walton, M. M., Tong, E. J., Sanchez, J. J., Kaiser, L. R., Stender, Y. O., Anderson, J. M., Ambrosino, C. M., Fernandez-Silva, I., Giuseffi, L. M., and Giambelluca, T. W.: The projected timing of climate departure from recent variability, *Nature*, 502, 183–187, doi:10.1038/nature12540, 2013. 2457
- Mueller, B. and Seneviratne, S. I.: Hot days induced by precipitation deficits at the global scale, *P. Natl. Acad. Sci. USA*, 109, 12398–12403, doi:10.1073/pnas.1204330109, 2012. 2458
- Müller, C., Waha, K., Bondeau, A., and Heinke, J.: Hotspots of climate change impacts in sub-Saharan Africa and implications for adaptation and development, *Glob. Change Biol.*, 20, 2505–2517, doi:10.1111/gcb.12586, 2014. 2466
- O’Neill, B. C., Krieglner, E., Riahi, K., Ebi, K. L., Hallegatte, S., Carter, T. R., Mathur, R., and Vuuren, D. P.: A new scenario framework for climate change research: the concept of shared socioeconomic pathways, *Climatic Change*, 122, 387–400, doi:10.1007/s10584-013-0905-2, 2013. 2474
- Olsson, L., Opondo, M., Tschakert, P., Agrawal, A., Eriksen, S. H., Ma, S., Perch, L. N., and Zakieldeen, S. A.: Livelihoods and poverty, in: *Climate Change 2014: Impacts, Adaptation, and Vulnerability. Part A: Global and Sectoral Aspects. Contribution of Working Group II to the Fifth Assessment Report of the Intergovernmental Panel of Climate Change*, edited by: Field, C. B., Barros, V. R., Dokken, D. J., Mach, K. J., Mastrandrea, M. D., Bilir, T. E., Chatterjee, M., Ebi, K. L., Estrada, Y. O., Genova, R. C., Girma, B., Kissel, E. S., Levy, A. N., MacCracken, S., Mastrandrea, P. R., and White, L. L., Cambridge University Press, Cambridge, UK, New York, NY, USA, 793–832, 2014. 2462, 2474
- Oppenheimer, M., Campos, M., Warren, R., Birkmann, J., Luber, G., O’Neill, B., and Kikkawa, T.: Emergent risks and key vulnerabilities, in: *Climate Change 2014: Impacts,*

**Climate impacts at
1.5 °C and 2 °C**

 C.-F. Schleussner et al.

[Title Page](#)
[Abstract](#)
[Introduction](#)
[Conclusions](#)
[References](#)
[Tables](#)
[Figures](#)

[Back](#)
[Close](#)
[Full Screen / Esc](#)
[Printer-friendly Version](#)
[Interactive Discussion](#)


Adaptation, and Vulnerability. Part A: Global and Sectoral Aspects. Contribution of Working Group II to the Fifth Assessment Report of the Intergovernmental Panel on Climate Change, edited by: Field, C. B., Barros, V. R., Dokken, D., Mach, K. J., Mastrandrea, M. D., Bilir, T. E., Chatterjee, M., Ebi, K. L., Estrada, Y., Genova, R., Girma, B., Kissel, E., Levy, A., MacCracken, S., Mastrandrea, P. R., and White, L., Cambridge University Press, Cambridge, UK, New York, NY, USA, chap. 19, 1039–1099, 2014. 2450

Orlowsky, B. and Seneviratne, S. I.: Global changes in extreme events: regional and seasonal dimension, *Climatic Change*, 110, 669–696, doi:10.1007/s10584-011-0122-9, 2012. 2457, 2458

Perrette, M., Landerer, F., Riva, R., Frieler, K., and Meinshausen, M.: A scaling approach to project regional sea level rise and its uncertainties, *Earth Syst. Dynam.*, 4, 11–29, doi:10.5194/esd-4-11-2013, 2013. 2467

Porter, J., Liyong, X., Challinor, A., Cochran, K., Howden, M., Iqbal, M., Lobell, D., and Travasso, M.: Food security and food production systems, in: IPCC 2014: Climate Change 2014: Impacts, Adaptation, and Vulnerability. Contribution of Working Group II to the Fifth Assessment Report of the Intergovernmental Panel on Climate Change, IPCC AR5 WGII, Cambridge University Press, Cambridge, New York, Chapter 7, 1–82, 2014. 2461

Pörtner, H.-O., Karl, D. M., Boyd, P. W., Cheung, W. W. L., Lluich-Cota, S. E., Nojiri, Y., Schmidt, D. N., and Zavialov, P.: Ocean systems, in: Climate Change 2014: Impacts, Adaptation, and Vulnerability. Part A: Global and Sectoral Aspects. Contribution of Working Group II to the Fifth Assessment Report of the Intergovernmental Panel on Climate Change, edited by: Field, C. B., Barros, V. R., Dokken, D., Mach, K. J., Mastrandrea, M. D., Bilir, T. E., Chatterjee, M., Ebi, K. L., Estrada, Y., Genova, R., Girma, B., Kissel, E., Levy, A., MacCracken, S., Mastrandrea, P. R., and White, L., Cambridge University Press, Cambridge, UK, New York, NY, USA, chap. 06, 411–484, 2014. 2472

Power, S., Delage, F., Chung, C., Kociuba, G., and Keay, K.: Robust twenty-first-century projections of El Niño and related precipitation variability, *Nature*, 502, 541–545, doi:10.1038/nature12580, 2013. 2473

Prudhomme, C., Giuntoli, I., Robinson, E. L., Clark, D. B., Arnell, N. W., Dankers, R., Fekete, B. M., Franssen, W., Gerten, D., Gosling, S. N., Hagemann, S., Hannah, D. M., Kim, H., Masaki, Y., Satoh, Y., Stacke, T., Wada, Y., and Wisser, D.: Hydrological droughts in the 21st century, hotspots and uncertainties from a global multimodel ensemble experiment, *P. Natl. Acad. Sci. USA*, 111, 3262–3267, doi:10.1073/pnas.1222473110, 2013. 2459

Climate impacts at 1.5 °C and 2 °C

C.-F. Schleussner et al.

Title Page

Abstract

Introduction

Conclusions

References

Tables

Figures



Back

Close

Full Screen / Esc

Printer-friendly Version

Interactive Discussion



- Riahi, K., Grübler, A., and Nakicenovic, N.: Scenarios of long-term socio-economic and environmental development under climate stabilization, *Technol. Forecast. Soc.*, 74, 887–935, doi:10.1016/j.techfore.2006.05.026, 2007. 2466
- Rignot, E., Mouginot, J., Morlighem, M., Seroussi, H., and Scheuchl, B.: Widespread, rapid grounding line retreat of Pine Island, Thwaites, Smith, and Kohler glaciers, West Antarctica, from 1992 to 2011, *Geophys. Res. Lett.*, 41, 3502–3509, doi:10.1002/2014GL060140, 2014. 2470
- Robinson, A., Calov, R., and Ganopolski, A.: Multistability and critical thresholds of the Greenland ice sheet, *Nature Climate Change*, 2, 429–432, doi:10.1038/nclimate1449, 2012. 2469, 2474
- Rogelj, J., Meinshausen, M., and Knutti, R.: Global warming under old and new scenarios using IPCC climate sensitivity range estimates, *Nature Climate Change*, 2, 248–253, doi:10.1038/nclimate1385, 2012. 2466
- Rogelj, J., McCollum, D. L., Reisinger, A., Meinshausen, M., and Riahi, K.: Probabilistic cost estimates for climate change mitigation, *Nature*, 493, 79–83, doi:10.1038/nature11787, 2013. 2466
- Rogelj, J., Meinshausen, M., Sedláček, J., and Knutti, R.: Implications of potentially lower climate sensitivity on climate projections and policy, *Environ. Res. Lett.*, 9, 031003, doi:10.1088/1748-9326/9/3/031003, 2014. 2466
- Rogelj, J., Luderer, G., Pietzcker, R. C., Kriegler, E., Schaeffer, M., Krey, V., and Riahi, K.: Energy system transformations for limiting end-of-century warming to below 1.5 °C, *Nature Climate Change*, 5, 519–527, doi:10.1038/nclimate2572, 2015. 2469, 2475
- Rosenzweig, C., Elliott, J., Deryng, D., Ruane, A. C., Müller, C., Arneth, A., Boote, K. J., Folberth, C., Glotter, M., Khabarov, N., Neumann, K., Piontek, F., Pugh, T. A. M., Schmid, E., Stehfest, E., Yang, H., and Jones, J. W.: Assessing agricultural risks of climate change in the 21st century in a global gridded crop model intercomparison, *P. Natl. Acad. Sci. USA*, 111, 3268–3273, doi:10.1073/pnas.1222463110, 2013. 2460, 2461, 2462, 2465, 2466
- Schaeffer, M., Hare, W., Rahmstorf, S., and Vermeer, M.: Long-term sea-level rise implied by 1.5 °C and 2 °C warming levels, *Nature Climate Change*, 2, 867–870, doi:10.1038/nclimate1584, 2012. 2468
- Schellnhuber, H.-J., Hare, W. L., Serdeczny, O., et al.: Turn down the heat: why a 4 °C warmer world must be avoided, *Tech. rep.*, The World Bank, Washington, DC, 2012. 2450

Climate impacts at 1.5 °C and 2 °C

C.-F. Schleussner et al.

[Title Page](#)
[Abstract](#)
[Introduction](#)
[Conclusions](#)
[References](#)
[Tables](#)
[Figures](#)

[Back](#)
[Close](#)
[Full Screen / Esc](#)
[Printer-friendly Version](#)
[Interactive Discussion](#)


Schellnhuber, H. J., Hare, B., Serdeczny, O., et al.: Turn down the heat: climate extremes, regional impacts, and the case for resilience, Main Report, The World Bank, Washington, DC, 2013. 2450, 2462

Schellnhuber, H. J., Reyer, C., Hare, B., et al.: Turn down the heat: confronting the new climate normal, Main Report, The World Bank, Washington, DC, 2014. 2450, 2475

Schewe, J., Heinke, J., Gerten, D., Haddeland, I., Arnell, N. W., Clark, D. B., Dankers, R., Eisner, S., Fekete, B. M., Colon-Gonzalez, F. J., Gosling, S. N., Kim, H., Liu, X., Masaki, Y., Portmann, F. T., Satoh, Y., Stacke, T., Tang, Q., Wada, Y., Wisser, D., Albrecht, T., Frieler, K., Piontek, F., Warszawski, L., and Kabat, P.: Multimodel assessment of water scarcity under climate change, *P. Natl. Acad. Sci. USA*, 111, 3245–3250, doi:10.1073/pnas.1222460110, 2013. 2459

Schleussner, C. F., Runge, J., Lehmann, J., and Levermann, A.: The role of the North Atlantic overturning and deep-ocean for multi-decadal global-mean-temperature variability, *Earth Syst. Dynam. Discuss.*, 4, 967–1003, doi:10.5194/esdd-4-967-2013, 2013. 2452

Schleussner, C.-F., Levermann, A., and Meinshausen, M.: Probabilistic projections of the Atlantic overturning, *Climatic Change*, 127, 579–586 2014. 2452

SED: UNFCCC: Report on the Structured Expert Dialogue (SED) on the 2013–2015 review, FCCC/SB/2015/INF.1, 2015. 2449

Sillmann, J., Kharin, V. V., Zhang, X., Zwiers, F. W., and Bronaugh, D.: Climate extremes indices in the CMIP5 multimodel ensemble: Part 2. Future climate projections, *J. Geophys. Res.-Atmos.*, 118, 2473–2493, doi:10.1002/jgrd.50188, 2013. 2457

Smith, K. R., Woodward, A., Campbell-Lendrum, D., Chadee, D., Honda, Y., Liu, Q., Olwoch, J., Revich, B., and Sauerborn, R.: Human health: impacts, adaptation, and co-benefits, in: *Climate Change 2014: Impacts, Adaptation, and Vulnerability. Contribution of Working Group II to the Fifth Assessment Report of the Intergovernmental Panel on Climate Change*, edited by: Field, C. B., Barros, V. R., Dokken, D., Mach, K. J., Mastrandrea, M. D., Bilir, T. E., Chatterjee, M., Ebi, K. L., Estrada, Y., Genova, R., Girma, B., Kissel, E., Levy, A., MacCracken, S., Mastrandrea, P. R., and White, L., Cambridge University Press, Cambridge, UK, New York, NY, USA, chap. 11, 709–754, 2014. 2457

Tai, A. P. K., Martin, M. V., and Heald, C. L.: Threat to future global food security from climate change and ozone air pollution, *Nature Climate Change*, 4, 817–821, doi:10.1038/nclimate2317, 2014. 2461

**Climate impacts at
1.5 °C and 2 °C**

 C.-F. Schleussner et al.

[Title Page](#)
[Abstract](#)
[Introduction](#)
[Conclusions](#)
[References](#)
[Tables](#)
[Figures](#)
[⏪](#)
[⏩](#)
[◀](#)
[▶](#)
[Back](#)
[Close](#)
[Full Screen / Esc](#)
[Printer-friendly Version](#)
[Interactive Discussion](#)


- Taylor, K. E., Stouffer, R. J., and Meehl, G. A.: An overview of CMIP5 and the experiment design, *B. Am. Meteorol. Soc.*, 93, 485–498, doi:10.1175/BAMS-D-11-00094.1, 2011. 2451
- Tebaldi, C. and Friedlingstein, P.: Delayed detection of climate mitigation benefits due to climate inertia and variability, *P. Natl. Acad. Sci. USA*, 110, 17229–17234, doi:10.1073/pnas.1300005110, 2013. 2453
- Tebaldi, C., Arblaster, J. M., and Knutti, R.: Mapping model agreement on future climate projections, *Geophys. Res. Lett.*, 38, L23701, doi:10.1029/2011GL049863, 2011. 2453
- Teh, L. S. L., Teh, L. C. L., and Sumaila, U. R.: A global estimate of the number of coral reef fishers, *PLoS ONE*, 8, e65397, doi:10.1371/journal.pone.0065397, 2013. 2473
- Timmermann, R. and Hellmer, H. H.: Southern Ocean warming and increased ice shelf basal melting in the twenty-first and twenty-second centuries based on coupled ice–ocean finite-element modelling, *Ocean Dynam.*, 63, 1011–1026, doi:10.1007/s10236-013-0642-0, 2013. 2470
- UNFCCC: (United Nations Framework Convention on Climate Change) (1992) Framework Convention on Climate Change, United Nations (UN), New York, 1992. 2449
- UNFCCC: Decision 1/CP.16. Report of the Conference of the Parties on its Sixteenth Session, held in Cancun from 29 November to 10 December 2010, Addendum, Part Two: Action taken by the Conference of the Parties at its Sixteenth Session, Decisions adopted by the Conference of the Parties. United Nations Framework Convention on Climate Change, Bonn, 2010. 2449
- Vaughan, M. M., Huffaker, A., Schmelz, E. a., Dafoe, N. J., Christensen, S., Sims, J., Martins, V. F., Swerbilow, J., Romero, M., Alborn, H. T., Allen, L. H., and Teal, P. E. a.: Effects of elevated [CO₂] on maize defence against mycotoxigenic *Fusarium verticillioides*, *Plant Cell Environ.*, 37, 2691–2706, doi:10.1111/pce.12337, 2014. 2461
- Wada, Y., van Beek, L. P. H., Sperna Weiland, F. C., Chao, B. F., Wu, Y.-H., and Bierkens, M. F. P.: Past and future contribution of global groundwater depletion to sea-level rise, *Geophys. Res. Lett.*, 39, 1–6, doi:10.1029/2012GL051230, 2012. 2468
- Warszawski, L., Frieler, K., Huber, V., Piontek, F., Serdeczny, O., and Schewe, J.: The Inter-Sectoral Impact Model Intercomparison Project (ISI-MIP): project framework, *P. Natl. Acad. Sci. USA*, 111, 3228–3232, doi:10.1073/pnas.1312330110, 2013. 2451, 2460
- Wigley, T. M. L. and Raper, S. C. B.: Extended scenarios for glacier melt due to anthropogenic forcing, *Geophys. Res. Lett.*, 32, L05704, doi:10.1029/2004GL021238, 2005. 2467

Winkelmann, R., Levermann, A., Ridgwell, A., and Caldeira, K.: Combustion of available fossil fuel resources sufficient to eliminate the Antarctic Ice Sheet, *Science Advances*, 1, e1500589, doi:10.1126/sciadv.1500589, 2015. 2474

5 Zhang, X., Alexander, L., Hegerl, G. C., Jones, P., Tank, A. K., Peterson, T. C., Trewin, B., and Zwiers, F. W.: Indices for monitoring changes in extremes based on daily temperature and precipitation data, *Wiley Interdisciplinary Reviews: Climate Change*, 2, 851–870, doi:10.1002/wcc.147, 2011. 2454

10 Zopa, S., Schulz, Y. B. M., and Cugnet, S. B. D.: Aerosol and ozone changes as forcing for climate evolution between 1850 and 2100, *Clim. Dynam.*, 40, 2223–2250, doi:10.1007/s00382-012-1408-y, 2012. 2452

ESDD

6, 2447–2505, 2015

Climate impacts at 1.5 °C and 2 °C

C.-F. Schleussner et al.

Title Page

Abstract

Introduction

Conclusions

References

Tables

Figures



Back

Close

Full Screen / Esc

Printer-friendly Version

Interactive Discussion



Table 1. Overview of the world regions used as well as the respective acronyms based on IPCC (2012). Please note that the Central American (CAM) region has been extended eastwards to also include the Caribbean.

ALA	Alaska, North-West Canada	NEB	North East Brazil
AMZ	Amazon	NEU	North Europe
CAM	Central America, Mexico, Caribbean	SAF	South Africa
CAS	Central Asia	SAH	Sahara
CEU	Central Europe	SAS	South Asia
CGI	East Canada, Greenland, Iceland	SAU	South Australia, New Zealand
CNA	Central North America	SEA	South-East Asia
EAF	East Africa	SSA	South-East South America
EAS	East Asia	TIB	Tibetan Plateau
ENA	East North America	WAF	West Africa
MED	Mediterranean	WAS	West Asia
NAS	North Asia	WNA	West North America
NAU	North Australia	WSA	West Coast South America

[Title Page](#)
[Abstract](#)
[Introduction](#)
[Conclusions](#)
[References](#)
[Tables](#)
[Figures](#)
[◀](#)
[▶](#)
[◀](#)
[▶](#)
[Back](#)
[Close](#)
[Full Screen / Esc](#)
[Printer-friendly Version](#)
[Interactive Discussion](#)


Climate impacts at 1.5 °C and 2 °C

C.-F. Schleussner et al.

Table 2. Projections for sea-level rise above the year 2000-levels for two illustrative 1.5 °C and 2 °C scenarios (see Fig. 13). Square brackets give the likely (66 %) range.

	1.5 °C	2 °C
SLR 2081–2100 [m]	0.37 [0.27,0.48]	0.44 [0.32,0.57]
SLR 2100 [m]	0.41 [0.29,0.53]	0.5 [0.36,0.65]
Rate of SLR 2041–2060 [mm year ⁻¹]	4.6 [3.2,5.8]	5.6 [4.0,7.0]
Rate of SLR 2081–2100 [mm year ⁻¹]	4.0 [2.7,5.5]	5.6 [3.8,7.7]

Title Page

Abstract

Introduction

Conclusions

References

Tables

Figures



Back

Close

Full Screen / Esc

Printer-friendly Version

Interactive Discussion



Climate impacts at 1.5 °C and 2 °C

C.-F. Schleussner et al.

Table 3. Fraction of reef cells at risk of long-term degradation due to coral bleaching in 2050 and 2100 for three different assumptions about the adaptive capacity and susceptibility of corals to ocean acidification as described in Sect. 7.1 in percent. Median projections and the 66 % range (in square brackets) are given, accounting for uncertainties in global mean temperature projections.

	1.5 °C	2 °C
2050		
Adaptation	9 [2,49]	39 [8,81]
Saturation	94 [60,100]	100 [95,100]
Constant	89 [48,99]	98 [86,100]
2100		
Adaptation	1 [0,2]	6 [1,50]
Saturation	69 [14,98]	100 [91,100]
Constant	69 [14,98]	99 [85,100]

[Title Page](#)
[Abstract](#)
[Introduction](#)
[Conclusions](#)
[References](#)
[Tables](#)
[Figures](#)

[Back](#)
[Close](#)
[Full Screen / Esc](#)
[Printer-friendly Version](#)
[Interactive Discussion](#)

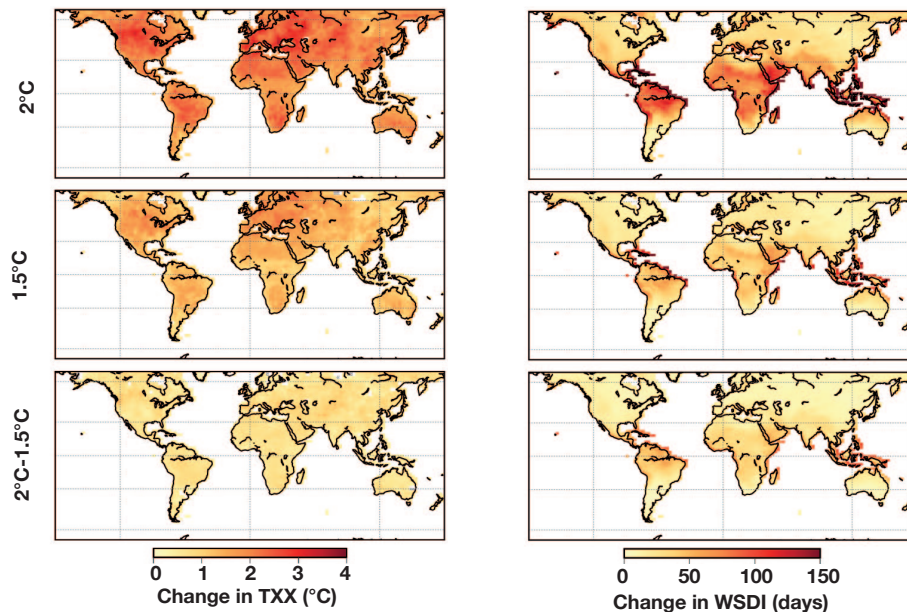



Figure 1. Median changes of TXx (left panels) and WSDI (right panels) for a warming of 2°C (upper panels), 1.5°C (middle panels) and the difference between the two warming levels (lower panels). Changes in TXx are given in °C, whereas changes in WSDI are given in days.

[Title Page](#)[Abstract](#)[Introduction](#)[Conclusions](#)[References](#)[Tables](#)[Figures](#)[◀](#)[▶](#)[◀](#)[▶](#)[Back](#)[Close](#)[Full Screen / Esc](#)[Printer-friendly Version](#)[Interactive Discussion](#)

Climate impacts at 1.5 °C and 2 °C

C.-F. Schleussner et al.

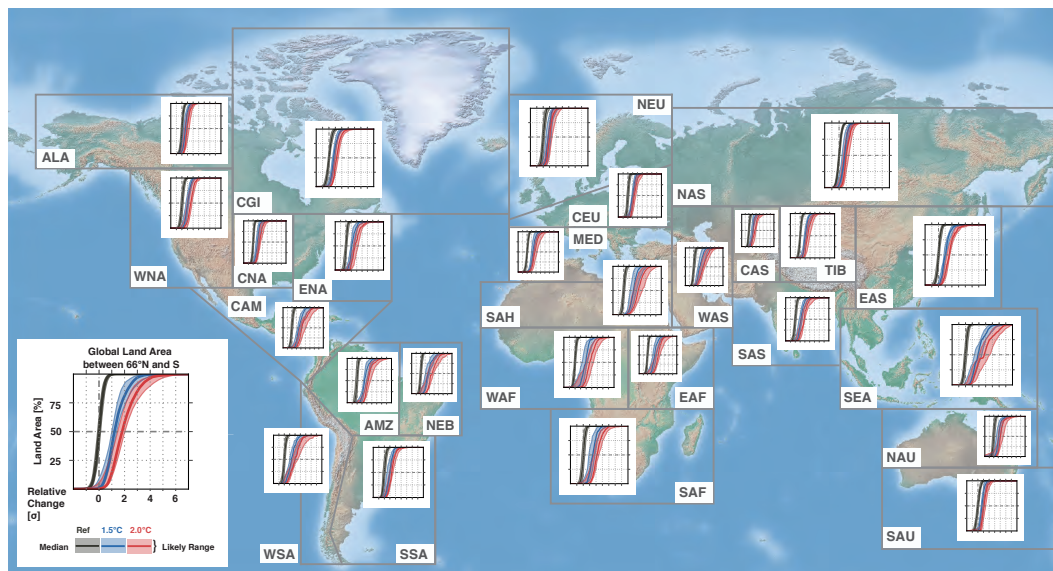


Figure 2. CDFs for projected regional aggregated changes for the global land area between 66° N and 66° S (lower left corner) as well as resolved for 26 world regions separately (see Sect. 2 for further details). Changes are given relative to the standard deviation over the 1986–2005 reference period. Note that a change in 2 (3) standard deviations implies that events with a reference return time of several decades (centuries) become the new normal, whereas a new normal of 4σ refers to an event that would be extremely unlikely to occur in a reference period climate.

Title Page

Abstract

Introduction

Conclusions

References

Tables

Figures



Back

Close

Full Screen / Esc

Printer-friendly Version

Interactive Discussion



ESDD

6, 2447–2505, 2015

Climate impacts at
1.5 °C and 2 °C

C.-F. Schleussner et al.

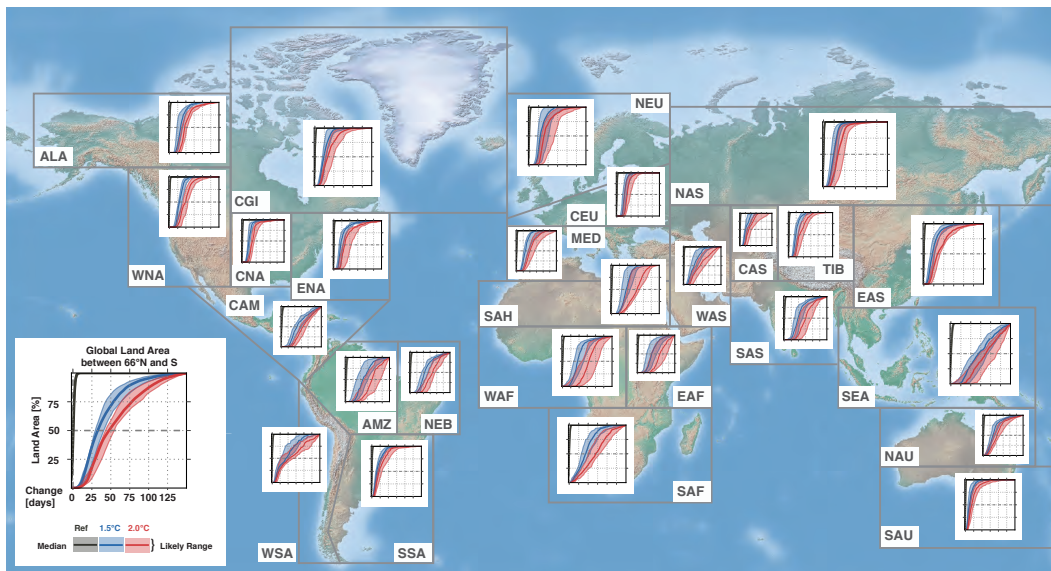


Figure 3. Same as Fig. 2, but for WSDI in days.

Title Page

Abstract

Introduction

Conclusions

References

Tables

Figures



Back

Close

Full Screen / Esc

Printer-friendly Version

Interactive Discussion



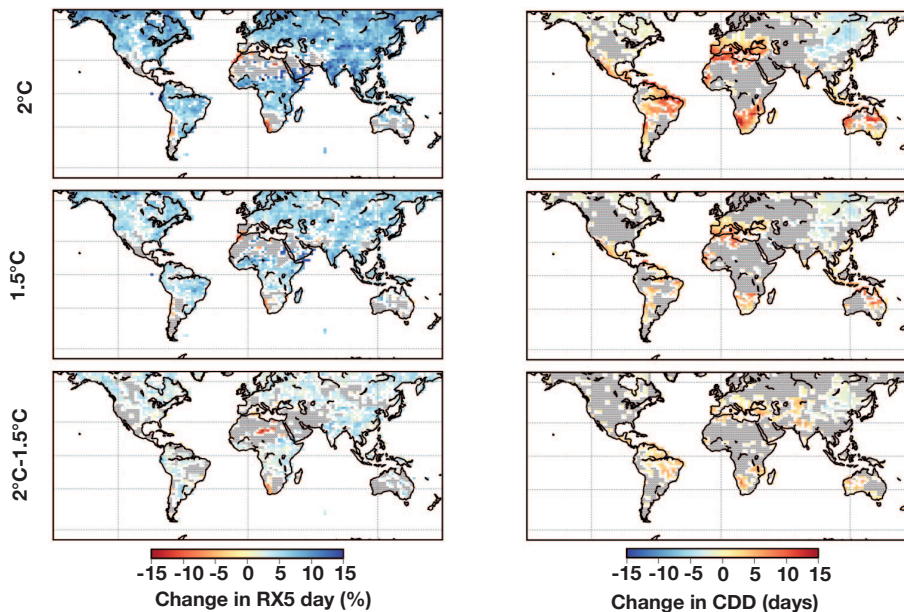


Figure 4. Same as Fig. 1, but for RX5day and CDD. Hatched areas indicate regions, where less than 66 % of the models in the ensemble agree with the sign of change of the median projections.

[Title Page](#)
[Abstract](#)
[Introduction](#)
[Conclusions](#)
[References](#)
[Tables](#)
[Figures](#)
[◀](#)
[▶](#)
[◀](#)
[▶](#)
[Back](#)
[Close](#)
[Full Screen / Esc](#)
[Printer-friendly Version](#)
[Interactive Discussion](#)


Climate impacts at 1.5 °C and 2 °C

C.-F. Schleussner et al.

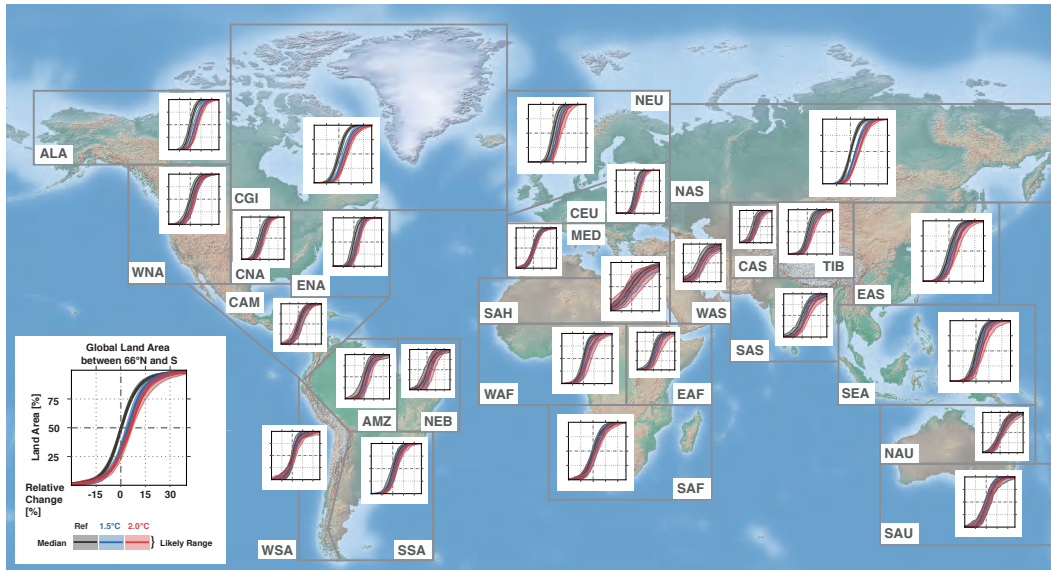


Figure 5. Same as Fig. 2 but for RX5day. Changes are given relative to the 1986–2005 reference period.

Title Page	
Abstract	Introduction
Conclusions	References
Tables	Figures
◀	▶
◀	▶
Back	Close
Full Screen / Esc	
Printer-friendly Version	
Interactive Discussion	



Climate impacts at 1.5 °C and 2 °C

C.-F. Schleussner et al.

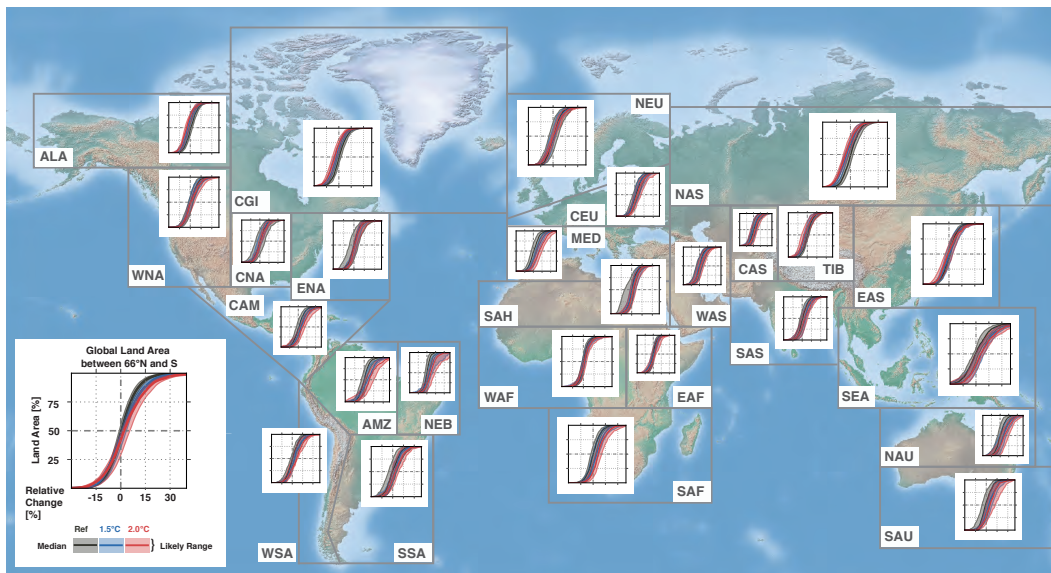


Figure 6. Same as Fig. 2 but for CDD. Changes are given relative to the 1986–2005 reference period.

[Title Page](#)
[Abstract](#)
[Introduction](#)
[Conclusions](#)
[References](#)
[Tables](#)
[Figures](#)

[Back](#)
[Close](#)
[Full Screen / Esc](#)
[Printer-friendly Version](#)
[Interactive Discussion](#)

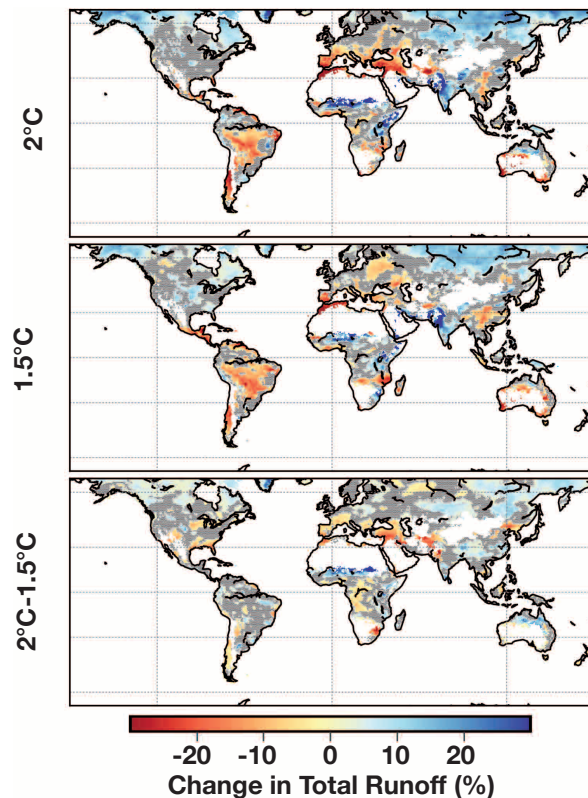



Figure 7. Median projections for changes in annual mean runoff for a warming of 2 °C (upper panel), 1.5 °C (middle panel) and the difference between both levels (lower panel) relative to the 1986–2005 reference period. The projections are based on the ISI-MIP GCM-GHM model ensemble. Grid cells where less than 66 % of all GCM-GHM pairs agree with the median sign of change are hatched out. Grid cells with an annual mean runoff of less than 0.05 mm day⁻¹ are masked white.

[Title Page](#)[Abstract](#)[Introduction](#)[Conclusions](#)[References](#)[Tables](#)[Figures](#)[◀](#)[▶](#)[◀](#)[▶](#)[Back](#)[Close](#)[Full Screen / Esc](#)[Printer-friendly Version](#)[Interactive Discussion](#)

Climate impacts at 1.5 °C and 2 °C

C.-F. Schleussner et al.

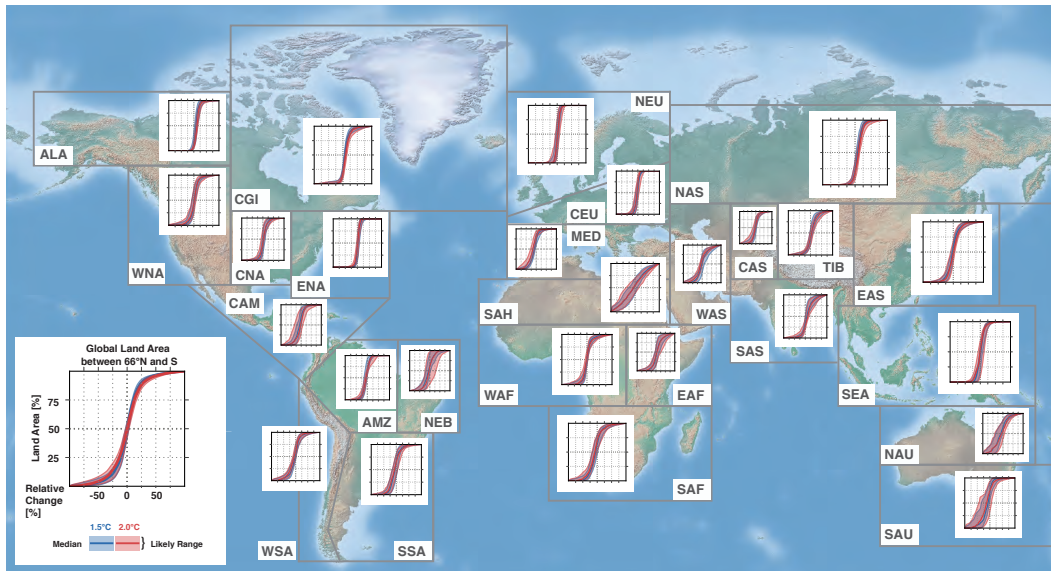


Figure 8. Same as Fig. 2 but for total annual runoff. Changes are given relative to the 1986–2005 reference period.

Title Page

Abstract

Introduction

Conclusions

References

Tables

Figures



Back

Close

Full Screen / Esc

Printer-friendly Version

Interactive Discussion



Climate impacts at 1.5 °C and 2 °C

C.-F. Schleussner et al.

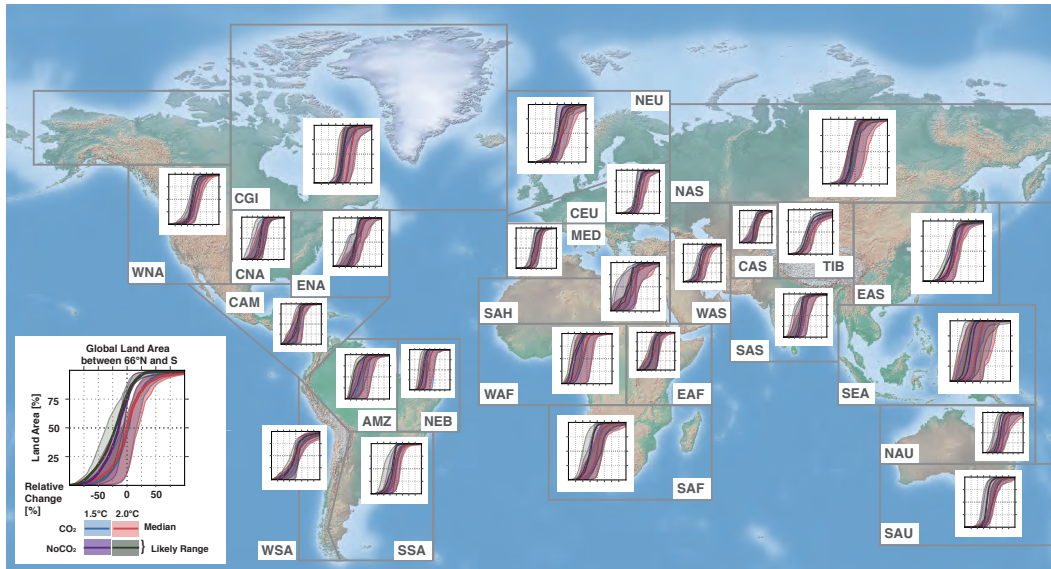


Figure 9. Same as Fig. 2 but for changes in wheat yields. Changes are given relative to the 1986–2005 reference period and ensemble projections excluding the effect of CO₂-fertilization are singled out explicitly. The CDFs are derived only over the present day growing areas of the crop (Monfreda et al., 2008).

[Title Page](#)
[Abstract](#)
[Introduction](#)
[Conclusions](#)
[References](#)
[Tables](#)
[Figures](#)

[Back](#)
[Close](#)
[Full Screen / Esc](#)
[Printer-friendly Version](#)
[Interactive Discussion](#)


ESDD

6, 2447–2505, 2015

Climate impacts at
1.5 °C and 2 °C

C.-F. Schleussner et al.

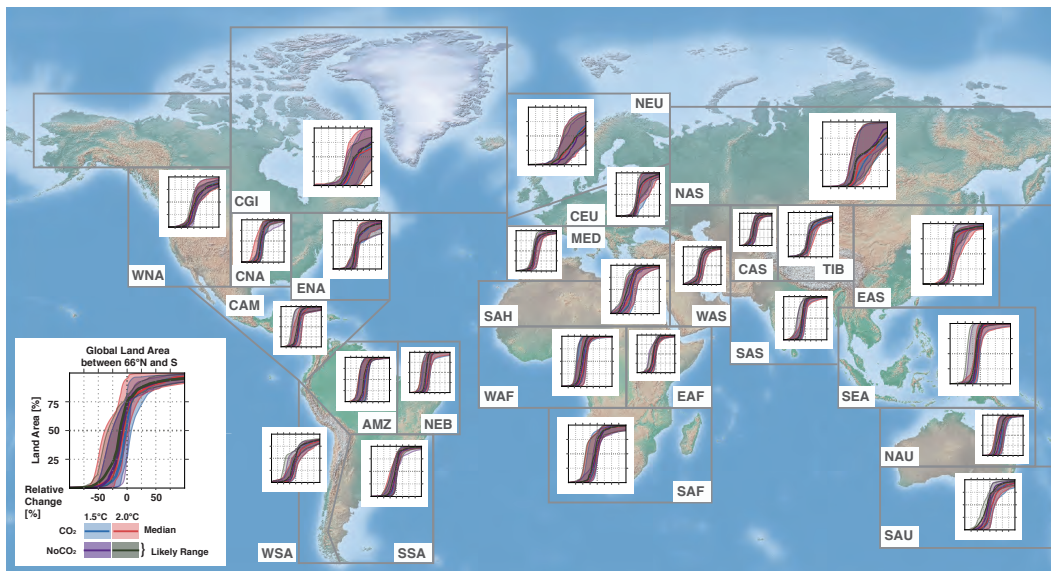


Figure 10. Same as Fig. 9, but for changes in maize yields.



Climate impacts at 1.5 °C and 2 °C

C.-F. Schleussner et al.

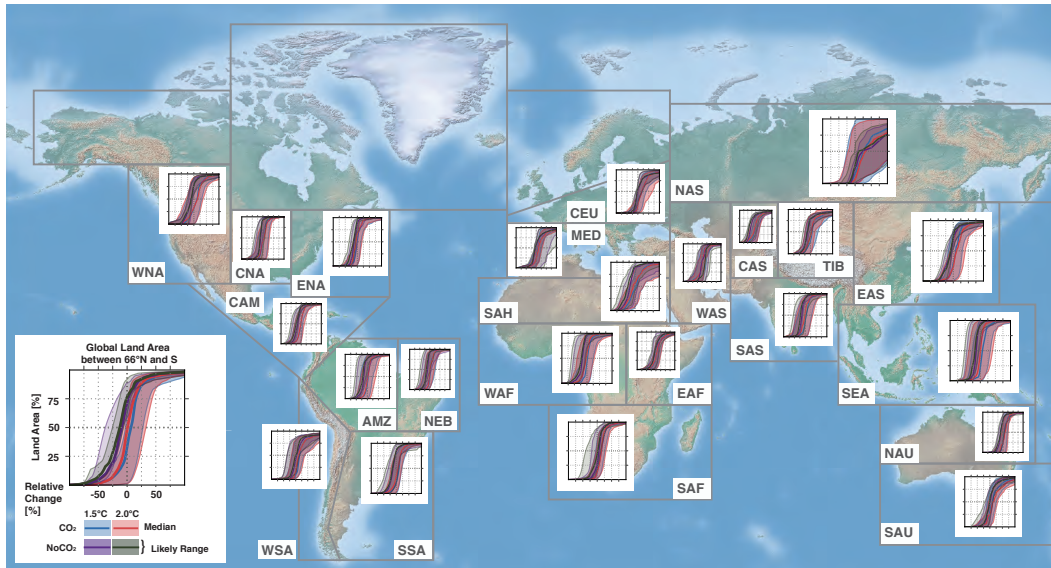


Figure 11. Same as Fig. 9, but for changes in soy yields.

Title Page

Abstract

Introduction

Conclusions

References

Tables

Figures

◀

▶

◀

▶

Back

Close

Full Screen / Esc

Printer-friendly Version

Interactive Discussion



ESDD

6, 2447–2505, 2015

Climate impacts at
1.5 °C and 2 °C

C.-F. Schleussner et al.

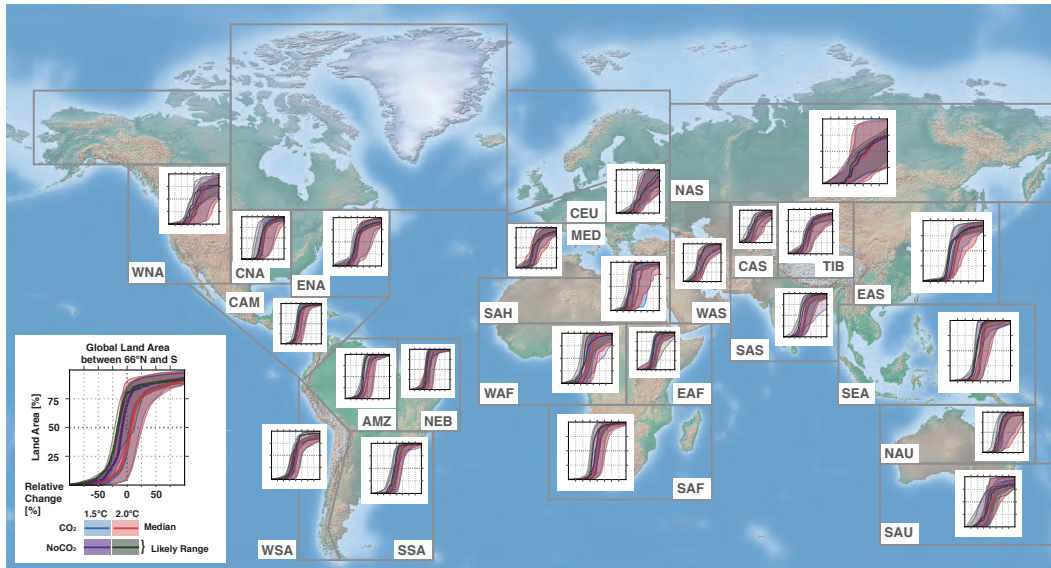


Figure 12. Same as Fig. 9 but for changes in rice yields.

Title Page

Abstract

Introduction

Conclusions

References

Tables

Figures

◀

▶

◀

▶

Back

Close

Full Screen / Esc

Printer-friendly Version

Interactive Discussion



Climate impacts at 1.5 °C and 2 °C

C.-F. Schleussner et al.

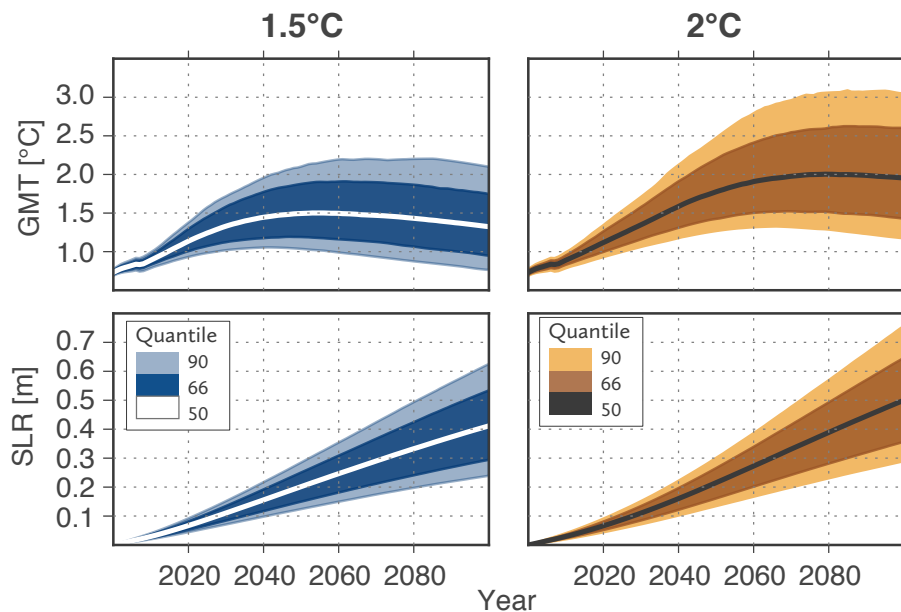


Figure 13. Upper panel: probabilistic GMT projections for illustrative emission scenarios with a peak warming of 1.5 °C (left panels) and 2 °C (right panels) above pre-industrial levels during the 21st century. Lower panels: probabilistic projections of global sea-level rise (SLR) for both scenarios relative to 1986–2005 levels. Uncertainty bands indicate the likely range (66 % probability within this range) and the very likely range (90 % probability), respectively.

[Title Page](#)
[Abstract](#)
[Introduction](#)
[Conclusions](#)
[References](#)
[Tables](#)
[Figures](#)
[◀](#)
[▶](#)
[◀](#)
[▶](#)
[Back](#)
[Close](#)
[Full Screen / Esc](#)
[Printer-friendly Version](#)
[Interactive Discussion](#)

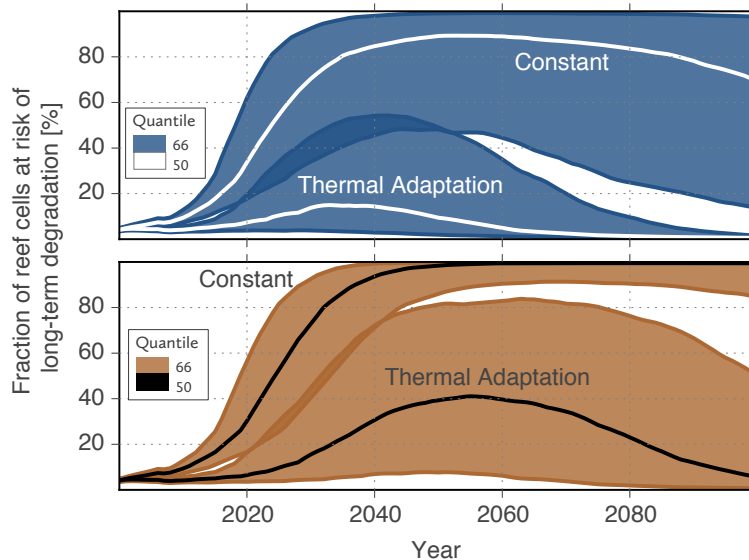



Figure 14. Probabilistic projections of the fraction of global tropical coral reef cells suffering from long-term degradation under two illustrative 1.5 °C (upper panel) and 2 °C (lower panel) scenarios (see Fig. 13 upper panel) for two different assumptions about the adaptive capacity following Frieler et al. (2012). Median projections and the 66 % range are shown. Note that uncertainties also include uncertainties in the GMT response (see Fig. 13). See Sect. 7.1 for further details on the methodology. Only the projections for the Constant and Adaptation scenario are shown, since the projections for the Saturation scenario differ only slightly from Constant. Table 3 gives results for all three scenarios assessed.

[Title Page](#)
[Abstract](#)
[Introduction](#)
[Conclusions](#)
[References](#)
[Tables](#)
[Figures](#)
[◀](#)
[▶](#)
[◀](#)
[▶](#)
[Back](#)
[Close](#)
[Full Screen / Esc](#)
[Printer-friendly Version](#)
[Interactive Discussion](#)
